JOURNAL OF NEUROPHYSIOLOGY
Vol. 71, No. 4, April 1994. *Printed in U.S.A.*

Physiological Properties of Anatomically Identified Axo-Axonic Cells in the Rat Hippocampus

E. H. BUHL, Z.-S. HAN, Z. LÖRINCZI, V. V. STEZHKA, S. V. KARNUP, AND P. SOMOGYI
Medical Research Council, Anatomical Neuropharmacology Unit, Oxford University, Oxford OX1 3TH, United Kingdom; and Department of Anatomy, University of Medicine and Pharmacy, 4300 Tirgu Mures, Romania

SUMMARY AND CONCLUSIONS

1. The properties of a well-defined type of GABAergic local circuit neuron, the axo-axonic cell ($n = 17$), were investigated in rat hippocampal slice preparations. During intracellular recording we injected axo-axonic cells with biocytin and subsequently identified them with correlated light and electron microscopy. Employing an immunogold-silver intensification technique we showed that one of the physiologically characterized cells was immunoreactive for γ-aminobutyric acid (GABA).

2. Axo-axonic cells were encountered in the dentate gyrus ($n = 5$) as well as subfields CA3 ($n = 2$) and CA1 ($n = 10$). They generally had smooth, beaded dendrites that extended throughout all hippocampal layers. Their axons ramified densely in the cell body layers and in the subjacent stratum oriens or hilus, respectively. Tested with electron microscopy, labeled terminals ($n = 53$) established synapses exclusively with the axon initial segment of principal cells in strata oriens and pyramidale and rarely in lower radiatum. Within a 400-μm slice a single CA1 axo-axonic cell was estimated to be in synaptic contact with 686 pyramidal cells.

3. Axo-axonic cells ($n = 14$) had a mean resting membrane potential of −65.1 mV, an average input resistance of 73.9 MΩ, and a mean time constant of 7.7 ms. Action potentials were of short duration (389-μs width at half-amplitude) and had a mean amplitude of 64.1 mV.

4. Nine of 10 tested cells showed a varying degree of spike frequency adaptation in response to depolarizing current injection. Current-evoked action potentials were usually curtailed by a deep (10.2 mV) short-latency afterhyperpolarization (AHP) with a mean duration of 28.1 ms.

5. Cells with strong spike frequency accommodation ($n = 5$) had a characteristic firing pattern with numerous spike doublets. These appeared to be triggered by an underlying depolarizing afterpotential. In the same cells, prolonged bursts of action potentials were followed by a prominent long-duration AHP with a mean time constant of 1.15 s.

6. Axo-axonic cells responded to the stimulation of afferent pathways with short-latency excitatory postsynaptic potentials (EPSPs) or at higher stimulation intensity with up to three action potentials. Axo-axonic cells in the dentate gyrus could be activated by stimulating the CA3 area as well as the perforant path, whereas in the CA1 area responses were elicited after shocks to the perforant path, Schaffer collaterals, and the stratum oriens-alveus border.

7. In the CA1 area the EPSP amplitude increased in response to membrane hyperpolarization. A more complex pattern of voltage sensitivity was apparent in the dentate gyrus. In CA1 cells bath-application of the *N*-methyl-D-aspartate (NMDA) receptor antagonist DL-2-amino-5-phosphonopentanoic acid ($n = 2$) had little or no effect on the control EPSP, whereas the non-NMDA receptor antagonist 6-cyano-7-nitroquinoxaline-2,3-dione ($n = 2$) resulted in a massive reduction of the EPSP amplitude. Thus axo-axonic cells receive glutamatergic excitatory input that is largely mediated by non-NMDA receptors.

8. Suprathreshold synaptic stimuli elicited inhibitory postsynaptic potentials (IPSPs) in axo-axonic cells. These were composed of an early $IPSP_A$ (peak latency 28.9 ms) that reversed at −66.5 mV and a late $IPSP_B$ (peak latency 124.8 ms) with a mean duration of 671 ms. This suggests that axo-axonic cells receive inhibitory GABAergic input.

9. In conclusion, axo-axonic cells reveal several response properties commonly associated with interneurons. However, despite their morphological homogeneity they display variability in their responses in vitro. Their synaptic activation suggests that all major hippocampal afferents can activate axo-axonic cells concomitantly with their postsynaptic principal cell targets.

BUHL

INTRODUCTION

Axo-axonic cells constitute a class of local circuit neurons that is unique to the cortex, including the hippocampal formation (reviewed in Somogyi 1989). Moreover, their widespread distribution in a variety of sensory and associational neocortical areas, in the hippocampal subfield CA1 as well as in the dentate gyrus (Fairen and Valverde 1980; Freund et al. 1983; Kisvarday et al. 1986; Marin-Padilla 1987; Somogyi 1977; Somogyi et al. 1983, 1985; Soriano and Frotscher 1989, Soriano et al. 1990) suggests that axo-axonic cells carry out an operation fundamental to the function of the cortical circuit. They are characterized by smooth or sparsely spinous dendrites, a feature which they however share with a variety of other local circuit cells. Like several other types of interneurons, axo-axonic cells utilize the neurotransmitter γ-aminobutyric acid (GABA), and thus it has been proposed that they may subserve an inhibitory role (Somogyi et al. 1985; Soriano and Frotscher 1989). The distinctiveness of the axo-axonic cell is therefore due to a high degree of synaptic target specificity. Axo-axonic cells exclusively innervate the axon initial segments of principal cells, that is, either pyramidal cells or granule cells of the dentate gyrus, respectively (Somogyi 1977; Somogyi et al. 1983; Soriano and Frotscher 1989; Soriano et al. 1990). Thus it appears that the output of interneurons can be regarded as their specific "signature."

In view of the rather strict layering of afferent as well as efferent pathways, the hippocampus is ideally suited for the study of principles of cortical synaptic organization. Indeed, in the dentate gyrus at least five highly distinct types of local circuit neurons may be discriminated (Han et al. 1993). Three of them pinpoint different segments of the granule cell's dendritic arbor and may thus be able to inter-

act locally and specifically with particular excitatory input synapses (Halasy and Somogyi 1993). In contrast, Ramon y Cajal's (1893) classical basket cell targets the cell body and dendritic stem and may therefore govern the somatic integration of inputs. Finally, the terminals of the axo-axonic cell are closest to the initiation site of the action potential and may thus control overall output and firing rate (Douglas and Martin 1990).

The anatomic complexity and diversity of local circuit neurons raises the obvious question of whether the selectivity in their connections is reflected in their physiological properties. The first progress in this direction was made by a number of studies on physiologically and, to some extent, morphologically identified interneurons, providing evidence that they may have membrane and firing properties that discriminate them from principal cells (Ashwood et al. 1984; Knowles and Schwartzkroin 1981; McCormick et al. 1985; Schwartzkroin and Kunkel 1985; Schwartzkroin and Mathers 1978). A short-duration action potential, a brief time constant, a deep, short-latency afterhyperpolarization, and little or no spike frequency adaptation are several of the features that were found to set interneurons apart from principal cells (recently reviewed in Connors and Gutnick 1990; Scharfman 1992). However, although interneurons may be grouped physiologically into a broad class of cells, subsequent studies have refined this view by providing evidence for their functional diversity. For example, in the hippocampal region CA1 it was recently recognized that interneurons in the pyramidal cell layer differed in their physiological properties from interneurons in the stratum lacunosum-moleculare (Kawaguchi and Hama 1987, 1988; Lacaille and Schwartzkroin 1988a). Moreover, the membrane properties of stratum oriens-alveus interneurons differ from the former two classes of local circuit cells (Lacaille and Williams 1990). Not only do these cells differ in their biophysical properties, but double recording experiments have also indicated differences in their effects on postsynaptic pyramidal cells. Thus stratum lacunosum-moleculare interneurons appear to evoke the late component of the inhibitory postsynaptic potential (IPSP; Lacaille and Schwartzkroin 1988b; Lacaille et al. 1989), whereas oriens-alveus and pyramidal cell layer interneurons may predominantly mediate the early phase of the IPSP (Knowles and Schwartzkroin 1981; Lacaille et al. 1987; Miles and Wong 1984; Miles 1990).

Although these findings indicate the physiological heterogeneity of interneurons, distinct subclasses such as the axo-axonic cell still await physiological characterization. Because their recognition requires light and electron microscopic analysis their physiological properties can only be evaluated in combination with intracellular labeling techniques. In the present study we pursued this strategy by employing recording electrodes containing biocytin and subsequently processing physiologically characterized hippocampal interneurons for correlated light and electron microscopy. From a large sample of morphologically diverse local circuit cells ($n > 80$) we extracted a total of 17 axo-axonic cells for subsequent analysis of their properties. Preliminary data has been presented in abstract form (Buhl et al. 1992).

METHODS

Slice preparation

Young adult female Wistar rats were deeply anesthetized with a mixture of inhaled ether and intramuscularly injected ketamine. The animals were intracardially perfused with ~30 ml of chilled artificial cerebrospinal fluid (ACSF). After perfusion the brain was quickly removed and transferred to a beaker with chilled, oxygenated ACSF. The brain was hemisected and after the frontal pole had been removed the cut end of the respective hemisphere was attached with cyanoacrylate glue to the stage of a vibroslice (Campden Instruments). Submerged in chilled ACSF, the tissue was sectioned at 400-μm thickness in the horizontal plane. Subsequently the hippocampus and temporal cortex were removed from the sections and transferred to an interface-type recording chamber where they were kept at 34–35°C on a nylon mesh at the interface between oxygenated ACSF and a humidified atmosphere saturated with 95% O_2-5% CO_2. The flow rate was maintained at 1.5 ml/min. Slices were allowed $\geq$1 h to equilibrate before recording. Normal ACSF was composed of (in mM) 126 NaCl, 3.0 KCl, 1.25 NaH_2PO_4, 24 $NaHCO_3$, 2.0 $MgSO_4$, 2.0 $CaCl_2$, and 10 glucose. During the initial stage (perfusion, cutting, and incubation) of most experiments the ACSF was modified according to Aghajanian and Rasmussen (1989) by replacing all NaCl (126 mM) with equimolar sucrose (252 mM). Thus passive chloride entry, which is presumed to be acutely responsible for neurotoxicity during slice preparation, is prevented. Only after 30 min of incubation in this modified ACSF was perfusion with normal ACSF started. On a subjective scale it appeared that the proportion and duration of viable recordings increased, whereas the physiological properties of neurons remained unchanged.

Intracellular recordings

Micropipettes were pulled from standard wall borosilicate tubing and filled with 2% biocytin (Horikawa and Armstrong 1988) in 1.5 M KCH_3SO_4. These electrodes were beveled to a final DC resistance of 80–150 MΩ. In the experiments recordings were obtained in the hilus or granule cell layer of the dentate gyrus and in the pyramidal cell layer of the Ammonic subfields CA3 and CA1. Cell types were classified on the basis of their physiological response properties. Putative interneurons were tentatively identified because of their distinct characteristics, such as short-duration action potentials, which were always followed by a deep short-latency afterhyperpolarization (AHP), a high rate of firing and, in several instances, only moderate spike frequency adaptation. Recordings were obtained with either an Axoclamp 2A or Axoprobe amplifier (Axon Instruments) operated in the bridge mode. Experimental data were digitized with a PCM instrumentation recorder adaptor and stored on videotapes. Data analysis was performed off-line with the aid of RC Electronics Computerscope software. Sampling rates varied between 1 and 10 kHz. Parameters are expressed as means ± SD.

Postsynaptic potentials were evoked with the use of bipolar tungsten electrodes (insulated in theta glass; 8 μm diam wire; tip separation ~50 μm) via a stimulus isolation unit. Because of the small dimensions of these electrodes it was possible to place them more accurately in particular pathways. Their high resistance (~1 MΩ) could require $\leq$40-V stimulation strength to elicit a maximal synaptic response. This would correspond to a current intensity of ~40 μA, which is well within the range reported by others.

Impalements not requiring the aid of steady hyperpolarizing current were accepted as stable recordings and could vary between 30 min and 6 h in duration. Biocytin was routinely ejected with 0.5-nA, 500-ms ON/OFF depolarizing pulses, although in several instances diffusion from the electrode tip during long-duration impalements could also result in strong labeling. As a result of the

prolonged depolarization the response of several neurons deteriorated markedly during dye iontophoresis. This often resulted in the total or partial loss of biocytin from cell bodies and dendrites, whereas the axon appeared remarkably well preserved as detected by subsequent histological examination. After dye filling we determined the membrane potential as the potential change on withdrawal of the pipette from the cell to the slice surface. When the recording time was <1 h the slices remained in the chamber for a further 30–60 min to allow sufficient transport of biocytin into the axon.

Histological processing

For fixation the slices were sandwiched between two Millipore filters and immersed overnight in 2.5% paraformaldehyde, 1.25% glutaraldehyde, and 15% (vol/vol) saturated picric acid in 0.1 M phosphate buffer (PB; 0.1 M) (Somogyi and Takagi 1982). On the following day the tissue was briefly rinsed in PB and infiltrated with 10% and 20% sucrose. Then the slices were snap-frozen in liquid nitrogen and thawed in PB. After gelatin embedding (for details see Buhl 1992) the slices were resectioned at 50- to 60-μm thickness with the aid of a vibratome. The tissue was washed 3 × 10 min with PB, followed by 2 × 10-min rinses in tris(hydroxymethyl)aminomethane (Tris) (0.05 M; pH 7.4)-buffered saline (TBS). Subsequently the sections were incubated for 1 h with 20% normal swine serum (NS) in TBS and then transferred to 1% avidin-biotinylated horseradish peroxidase complex (ABC; Vector Laboratories) in TBS with 1% NS added, where they remained overnight at 4°C.

Unbound ABC was removed by 3 × 20-min washes in TBS and 2 × 20-min washes in Tris buffer (TB; pH 7.6) and then the sections were reacted for ~10 min in TB with 0.05% 3,3-diaminobenzidine tetrahydrochloride (DAB) and 0.01% hydrogen peroxidase added. After excess DAB had been washed out with TB (1 × 15 min) and PB (2 × 10 min) the sections were postfixed with 1% osmium tetroxide dissolved in PB. The tissue was then transferred to PB, washed 3 × 10 min in distilled water and block-stained with a 1% aqueous solution of uranyl acetate. After two further rinses in distilled water the sections were flattened between a slide and coverslip and subsequently dehydrated in an ascending series of ethanol. After 2 × 10 min in propylene oxide the material was infiltrated overnight with Durcupan (Fluka). On the following day the sections were spread out on a slide and mounted under a coverslip. The resin was polymerized for 48 h at 60°C.

After light microscopic analysis we reembedded tentatively identified axo-axonic cells for electron microscopic purposes (for details see Somogyi and Takagi 1982). Labeled terminal branches of the axon were traced in serial sections to determine their postsynaptic targets. Ultrathin sections containing labeled terminal branches of a CA3 axo-axonic cell were immunostained with an antiserum directed against GABA using the same antiserum, controls, and a sensitive immunogold-silver intensification procedure as described earlier (Halasy and Somogyi 1993).

RESULTS

Anatomic identification of axo-axonic cells

Intracellularly recorded and biocytin-filled neurons were scrutinized with light microscopy for the presence of the following features: *1*) smooth or sparsely spinous dendrites; *2*) the axonal arbor mainly distributed in the lower half of the principal cell layer and the subjacent zone, i.e., upper stratum oriens or the polymorphic layer of the hilus, respectively; and *3*) most importantly, terminal branches of the axon forming radially oriented rows (Figs. 1, 2, and 3, *A* and *B*). On the basis of these criteria 17 cells were tentatively identified as axo-axonic cells. From these, 5 were located in the dentate gyrus, 2 in the CA3 region, and the remaining 10 in subfield CA1. In several instances a slice could also contain one or two labeled principal cells that were in close proximity to the filled axo-axonic cell, even when only one cell with the unmistakable electrophysiological characteristics of an interneuron had been recorded. This multiple labeling was attributed to some of the tracer diffusing into adjoining principal cells after the withdrawal of the recording electrode. Conversely, it seems rather unlikely that a pyramidal cell recording would display distinct interneuronal properties and concomitantly result in the spurious filling of one of the numerically sparse local circuit neurons. This is corroborated by the finding that numerous recordings that displayed the electrophysiological characteristics of principal cells did not result in the filling of axo-axonic or any other local circuit cells.

Subsequently we reembedded pieces of axo-axonic cells ($n = 9$) from all three regions for electron microscopy to verify whether their terminal boutons established synapses with the axon initial segment of principal cells. Altogether 53 labeled synaptic terminals were identified and they formed symmetrical synapses exclusively with the axon initial segment of principal cells. These results provide further evidence that axo-axonic cells may be readily discriminated because of their distinctive light microscopic features (Li et al. 1992; Somogyi et al. 1983, 1985) and in our hands the light microscopic prediction unequivocally identified these neurons. It appeared therefore unnecessary to scrutinize the remaining eight cells at the electron microscopic level.

Morphological features of axo-axonic cells

The anatomy of axo-axonic cells in the dentate gyrus (Halasy and Somogyi 1993; Han et al. 1993; Soriano and Frotscher 1989; Soriano et al. 1990) and subfield CA1 of Ammon's horn (Li et al. 1992a; Somogyi et al. 1983, 1985) has been addressed previously. In these studies a number of discrepancies are apparent (e.g., the extent and distribution of the axon) but these are largely attributable to differences in visualization methods. Because the present paper is largely concerned with the physiological properties of axo-axonic cells only the most salient, novel, or physiologically relevant anatomic data will be summarized.

In general the dendrites of axo-axonic cells were varicose and smooth, although they occasionally displayed a few spines (Fig. 1). Usually the cells gave rise to several primary dendrites that ramified further into secondary and tertiary branches. In all hippocampal subfields a tuft of apically directed dendrites invaded the molecular layer (here understood as either the dentate molecular layer or the combined strata radiatum and lacunosum moleculare in Ammon's horn), frequently reaching the hippocampal fissure. In the CA1 area a prominent tuft seems to be a feature that distinguishes axo-axonic cells from other stratum pyramidale interneurons (Buhl and Somogyi, unpublished data). Interestingly, one axo-axonic cell in the hilar part of subfield CA3 (CA3c) had several dendrites that penetrated the granule cell layer and advanced into the dentate molecular layer (Fig. 2*B*). Thus axo-axonic cells may be predisposed to receiving entorhinal and commissural associational input

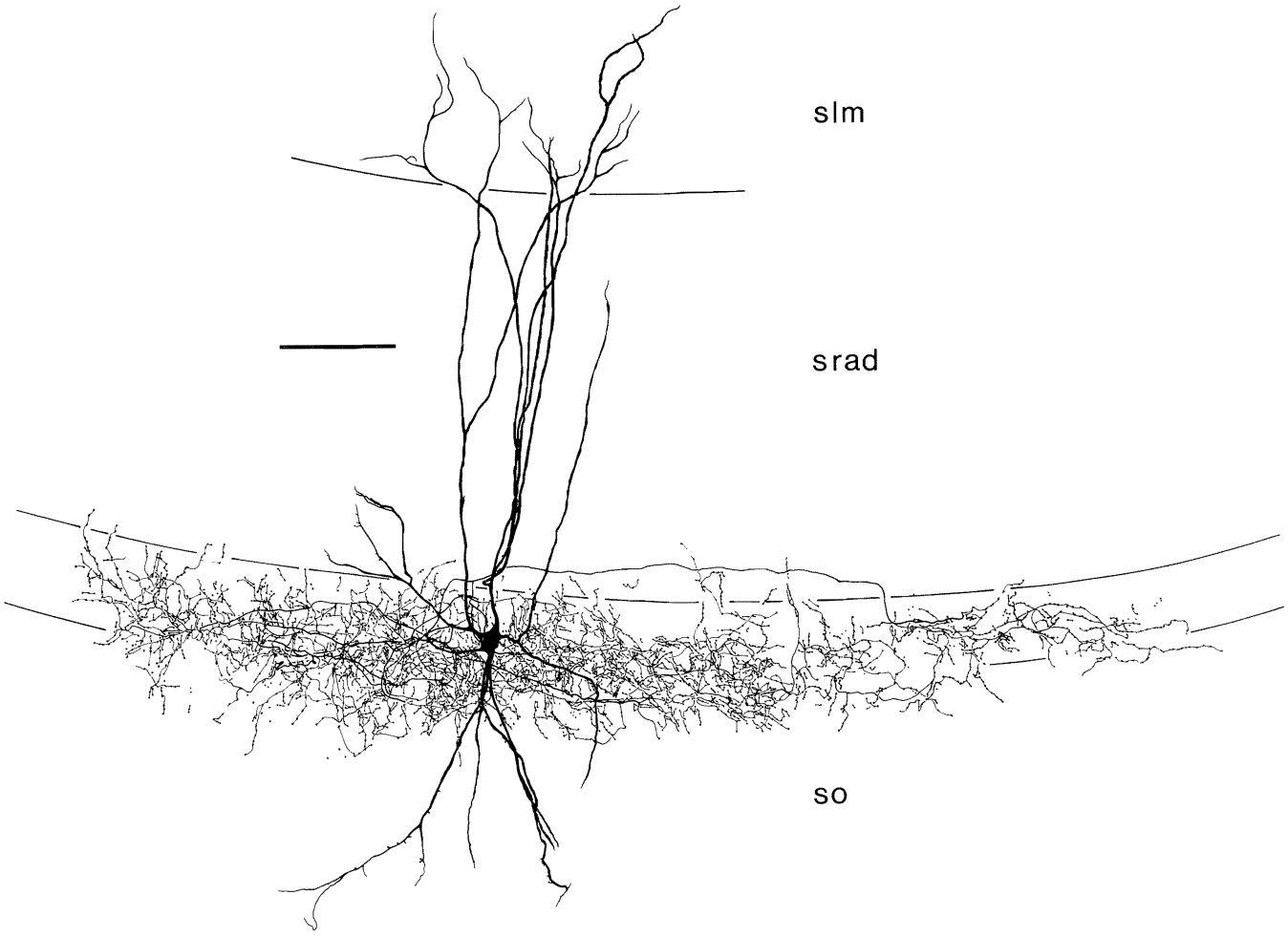

FIG. 1. Intracellularly recorded and biocytin-filled axo-axonic cell in subfield CA1 of the rat hippocampus. The cell was reconstructed with light microscopy from 5×60-μm-thick sections. The cell body that was located in the pyramidal cell layer (between ——) gave rise to several dendrites that traversed stratum radiatum (srad) and formed a characteristic apical tuft in the stratum lacunosum moleculare (slm). A skirt of basal dendrites coursed through the stratum oriens (so), with their tips protruding into the alveus. The axon, which was only partially filled, formed a dense band of terminal branches in the lower half of and subjacent to the pyramidal cell layer. Properties of this cell are also shown in Figs. 4*A*, 6*A*, 10*A*, and 11, *A*, *C*, and *D*. Scale bar = 100 μm.

in the dentate gyrus, whereas in the CA1 area they may be contacted both by entorhinal afferents and the Schaffer collaterals originating in the CA3 area. Apart from their apical tuft, axo-axonic cells had slightly fewer basal dendrites that ramified in the hilus in the dentate or traversed the stratum oriens in Ammon's horn and invaded the superficial part of the alveus (Fig. 1). Therefore these dendrites may be selectively targeted by recurrent collaterals of granule cells or pyramidal cells, respectively.

The main axon usually emerged from the cell body, giving rise to several main branches (Figs. 1, 2, and 3*A*). These were frequently myelinated (Fig. 3*D*) and ramified above the cell body layer, then, taking a course parallel to the latter, traversed the lower part of the molecular layer. Eventually they gave rise to a dense network of terminal branches that were studded with numerous boutons (Fig. 3, *A* and *B*). Characteristically the axonal arbor was highly laminated, occupying the lower half of the cell body layer and either the upper third of the stratum oriens or the subgranular hilus, respectively. Occasional varicosity-bearing collaterals in the stratum radiatum (Figs. 1 and 2) appeared to be aligned with the axons of ectopic pyramidal cells. We subsequently confirmed the correctness of this prediction by investigating one such branch in the stratum radiatum of area CA1 in serial ultrathin sections. Three boutons were studied, all of which were in synaptic contact with a pyramidal cell axon initial segment. In Ammon's horn the maximal extent of the axonal arbor (within the horizontal plane) was determined to be 950 μm, whereas a dentate gyrus cell spread $\leq$1.1 mm along the granule cell layer. As an additional feature, all (n = 5) hilar dentate axo-axonic cells supplied large portions of the hilus with a dense meshwork of fibers, thus confirming the findings of Han et al. (1993). Axo-axonic terminal branches were largely composed of distinct, orderly rows or fascicles of boutons that ran perpendicular to the laminar boundaries (Fig. 3, *A* and *B*). This feature was most conspicuous in the dentate gyrus (Fig. 3*A*), whereas many of the terminal rows in Ammon's horn showed more oblique trajectories (Figs. 1, 2, and 3*B*), presumably reflecting more divergent trajectories taken by the axon initial segment of pyramidal cells.

For the axo-axonic cell illustrated in Fig. 1 a quantitative

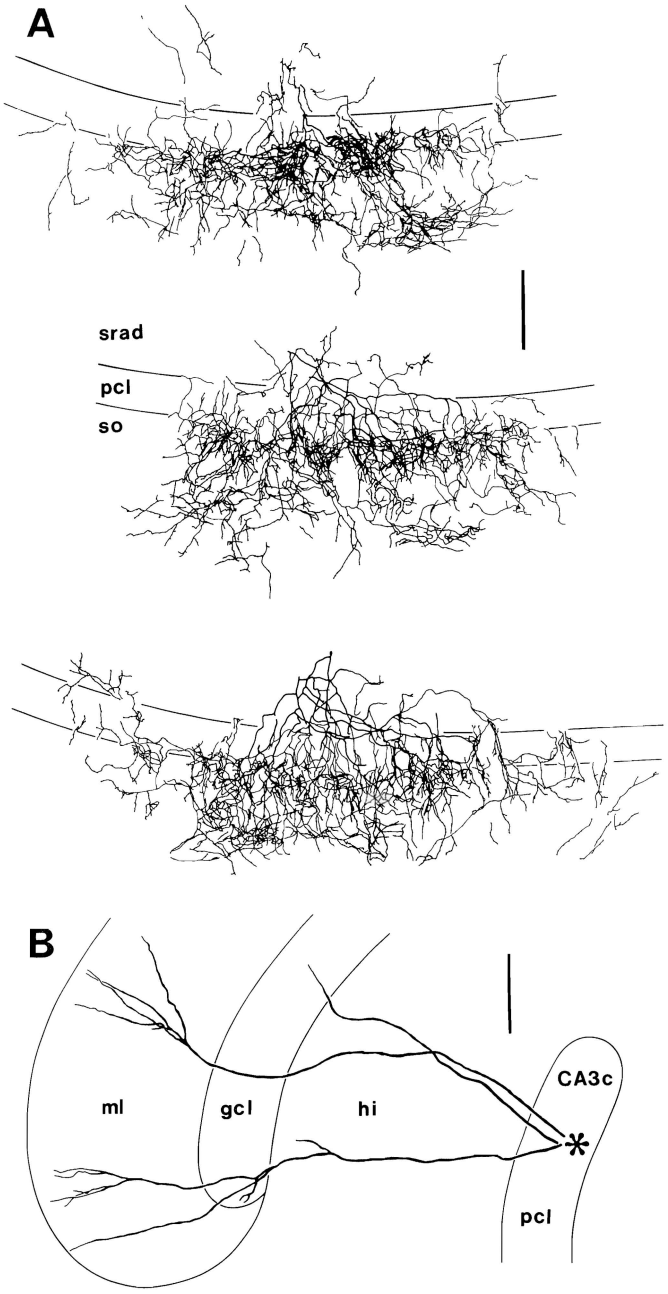

FIG. 2. *A*: axon of a physiologically characterized axo-axonic cell in area CA1. Because the axonal arbor of this cell was too dense to be represented by a composite drawing, the axon that was originally contained in a 400-μm-thick slice was reconstructed at 4 separate levels (3 shown here) that can be superimposed on the pyramidal cell layer (pcl). This cell was located at the subicular end of the CA1 area, where pyramidal cells form a compact layer below the stratum radiatum and an additional tier of more loosely arranged cells in the stratum oriens. This particular distribution pattern is reflected in the arrangement of axo-axonic terminal branches, which was also found in the lower stratum oriens. Note that terminal branches may take a rather oblique course, which reflects the trajectory of pyramidal cell axons. *B*: dendrites of an axo-axonic cell that was located in the hilar sector of subfield CA3 (CA3c). All primary dendrites could be traced through the hilus (hi) to the remnants of the cell body (*) in the pyramidal cell layer, which had disintegrated during the postfilling incubation period. The axon, however, remained intact and was subsequently verified to establish symmetrical synapses with the axon initial segment of CA3 pyramidal cells (Fig. 3). Note that several dendrites traverse the granule cell layer (gcl) and branch profusely in the molecular layer (ml) of the dentate gyrus. Scale bars = 100 μm.

estimate was made to determine the number of postsynaptic pyramidal cells. Previous electron microscopic evidence (Somogyi et al. 1983, 1985) indicated that in Ammon's horn one cluster of terminals is predominantly associated with one initial segment only. Thus a count of terminal segments consisting of varicosities suggested that 686 (corrected for the segments cut on the surface of sections) pyramidal cells received input from one axo-axonic cell within the 400-μm-thick slice.

Postsynaptic targets

In the electron microscope, biocytin labeled profiles were readily identified because of their content of an opaque reaction product. Vesicle-containing boutons established exclusively symmetrical (type 2) synaptic contacts with their respective postsynaptic targets (Fig. 3, *C* and *F*). These were all identified as axon initial segments because of the presence of an electron dense membrane undercoating and/or fascicles of microtubules. However, differences were observed in the fine structural characteristics of the axon initial segments when compared with those obtained from perfusion-fixed brains. With increasing in vitro survival time the undercoating tended to diminish and the microtubule fascicles generally separated into individual microtubules. From a total of nine cells 53 synapses were identified as forming axo-axonic synaptic junctions with axon initial segments. None of the tested biocytin-filled boutons made synapses with any other target, i.e., somata or dendrites, even when these were in direct membrane apposition to the bouton. Some axo-axonic cells had rows of boutons in lower stratum radiatum in the CA1 area (Fig. 2*A*). To establish their postsynaptic targets we serially sectioned one row from the axon shown in Fig. 2 and studied it with electron microscopy. The row of boutons followed an axon initial segment and three of the boutons could be shown to form synaptic junctions with it. Such initial segments probably belong to disoriented axons or they derive from ectopic pyramidal cells located in stratum radiatum. These findings confirm the notion that the output of axo-axonic cells is highly specific, and beyond, that their light microscopic features are sufficiently distinctive to permit their unequivocal identification. Therefore the remainder of eight cells was accepted without being scrutinized in the electron microscope.

GABA immunoreactivity of identified axo-axonic cells

There is evidence that in slices maintained under in vitro conditions the overall amount of GABA gradually decreases during the incubation period (Mihaly et al. 1991). In slice material conventional postembedding methods for the immunocytochemical demonstration of GABA that employ secondary antibodies conjugated to 5- to 40-nm gold particles may thus result in a low signal-to-noise ratio. These technical difficulties were resolved by using a 1-nm gold conjugated secondary antiserum and visualizing the latter by silver intensification (for detailed discussion and control reactions see Halasy and Somogyi 1993). When visualized in the electron microscope, biocytin-filled GABA-positive terminals were characterized by large ovoid

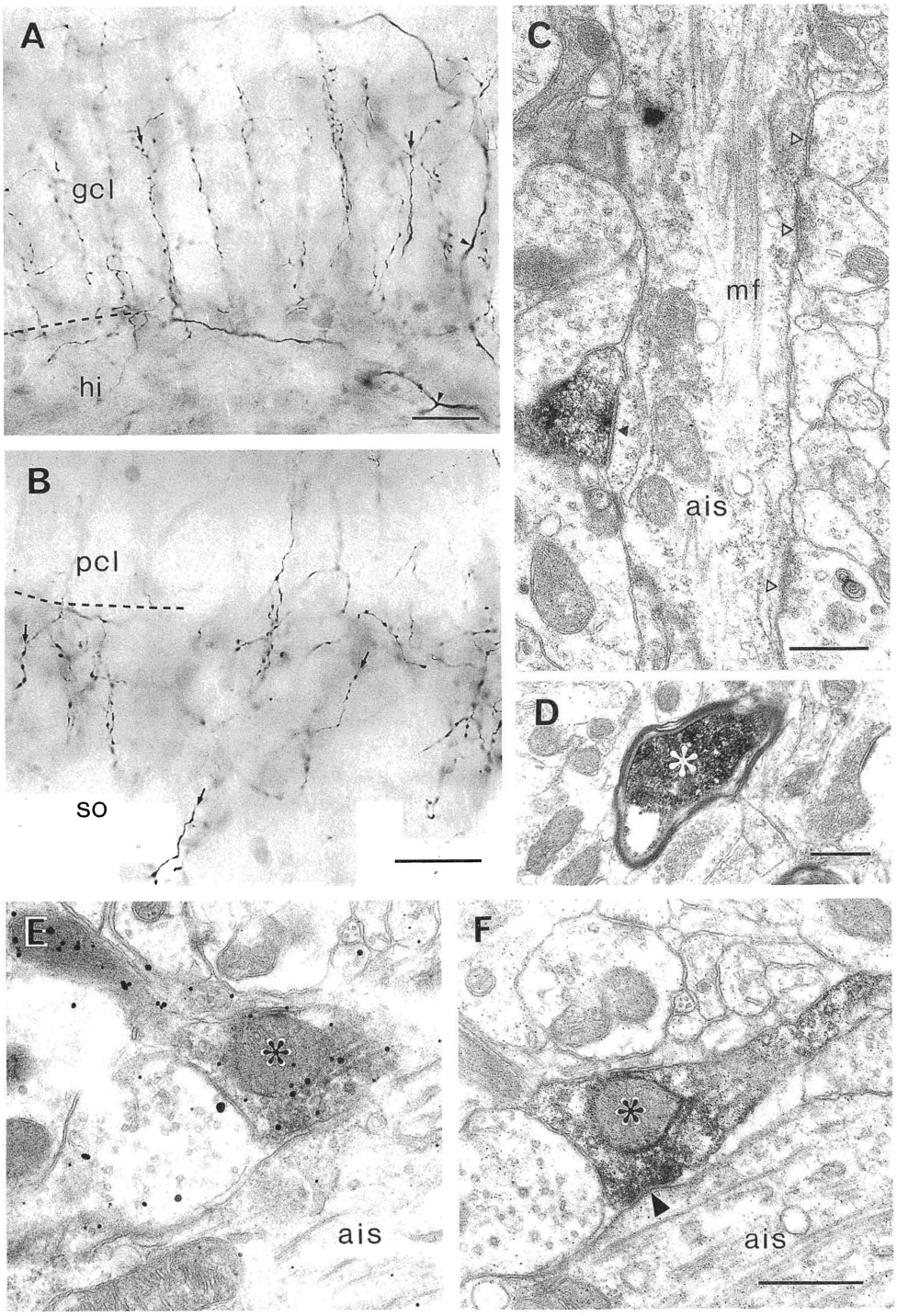

FIG. 3. *A* and *B*: terminal branches (↓) of axo-axonic cells have a distinct light microscopic appearance. They are composed of bouton-studded terminal rows that run perpendicular to the boundaries of either the granule cell layer or the pyramidal cell layer. When compared with subfield CA1 (*B*) the arrangement of terminals in the dentate gyrus (*A*) are more orderly, reflecting axonal trajectories of the principal cells. Arrowheads in *A*: main branches of the axon. *C*: identified terminal of an axo-axonic cell in subfield CA3, which established a symmetrical synapse (▲) with an axon initial segment (ais). The latter is identified by its fine structural characteristics, such as the presence of microtubule fascicles (mf). Unlabeled terminals of similar character were also found in synaptic contact (△) with the same initial segment, indicating the convergence of several axo-axonic cells on 1 common target. *D*: main branches of axo-axonic cell axons (white asterisk) were frequently myelinated. *E* and *F*: serial sections of a synaptic bouton (*) of the axo-axonic cell shown in *C* and *D*. The section in *E* was reacted to reveal γ-aminobutyric acid (GABA) immunoreactivity using a silver intensification immunogold method. The high density of electron dense metal particles over the labeled and neighboring boutons demonstrates that they contain GABA. The unreacted section in *F* demonstrates the synaptic contact (arrowhead). Scale bars in *A* and *B* = 15 μm; in *C–F* = 0.5 μm. *E* and *F* at same magnification. The cell shown in *C–F* is illustrated in Fig. 2*B*.

vesicles and were selectively labeled with irregularly shaped silver-intensified gold particles (Fig. 3*E*).

Membrane properties

Recordings were judged acceptable for the analysis of membrane properties when cells had a stable resting membrane potential (RMP) exceeding −55 mV without requiring steady hyperpolarizing current injection. Thus, from a total of 17 cells, 3 cells were subsequently rejected from analysis. Apart from being relatively depolarized, these cells showed other signs of neuronal injury, such as low input resistance or wide and low-amplitude action potentials. The remainder (n = 14) had a mean RMP of −65.1 ± 3.9 (SD) mV, ranging from −59 to −73 mV.

Membrane time constants were calculated from averages of typically 0.1-nA, 200-ms hyperpolarizing pulses as the time necessary to reach e^{-1} (63%) of the maximum voltage deflection. Axo-axonic cells had a mean time constant of 7.7 ± 3.8 ms, ranging from 3.1 to 17.1 ms. The input resistance of the cells was determined from averages of 0.1-nA, 200-ms hyperpolarizing pulses (Fig. 4*A*). Measurements were taken at the plateau of the voltage response and ranged from 38 to 116 MΩ. They were, on average, 73.9 ± 23.8 MΩ. When we injected families of hyper- and depolarizing current pulses, the majority of axo-axonic cells showed no inward rectification in either hyper- or depolarizing direction (tested between firing threshold and approximately −100 mV membrane potential). Diverging from this general pattern, one hilar axo-axonic cell showed a decrease of its membrane resistance from 70 to 55 MΩ when being hyperpolarized (Fig. 9*D*). Occasionally cells showed a small sag in the later part of the voltage response, indicating a modest degree of time-dependent inward rectification (Fig. 9*C*). Anodal break excitation was usually absent.

Firing properties

ACTION POTENTIAL. In contrast to pyramidal cells, axo-axonic cells have nonovershooting action potentials with a mean amplitude of 64.1 ± 7.1 mV (n = 13) when measured from baseline. Measured at half-amplitude, action potentials had a mean duration of 389 ± 86 μs, which was largely due to a relatively high rate of fall, being only marginally slower than their rate of rise (Fig. 4*B*). Apart from one cell in the CA3 area, axo-axonic cells rarely fired spontaneously. Several cells did, however, display numerous spontaneous synaptic events, which differed markedly from concomitantly recorded excitatory postsynaptic potentials (EPSPs) in pyramidal cells because of their fractionated appearance (Fig. 4*D*).

REPETITIVE FIRING. The presence of spike frequency adaptation was investigated in 10 axo-axonic cells by injecting 0.1- to 0.7-nA, 200-ms and/or 500-ms depolarizing current pulses (Fig. 5). In one cell the rate of firing increased by 17%, whereas the remainder (n = 9) exhibited various degrees of spike frequency adaptation. When the decline in the firing rate is expressed as the percentage difference between the first and last interspike interval, the decrement in the rate of firing could vary between 2.5% and 81%, with a mean of 39.4 ± 28.0%. This variability in the reduction of the firing rate is illustrated in Fig. 5, which shows the difference between an almost nonadapting dentate gyrus cell (Fig. 5, *A–C*) and a strongly adapting cell in subfield CA1 (Fig. 5, *D–F*). Interestingly, the mode of adaptation in the most strongly accommodating axo-axonic cells in subfield

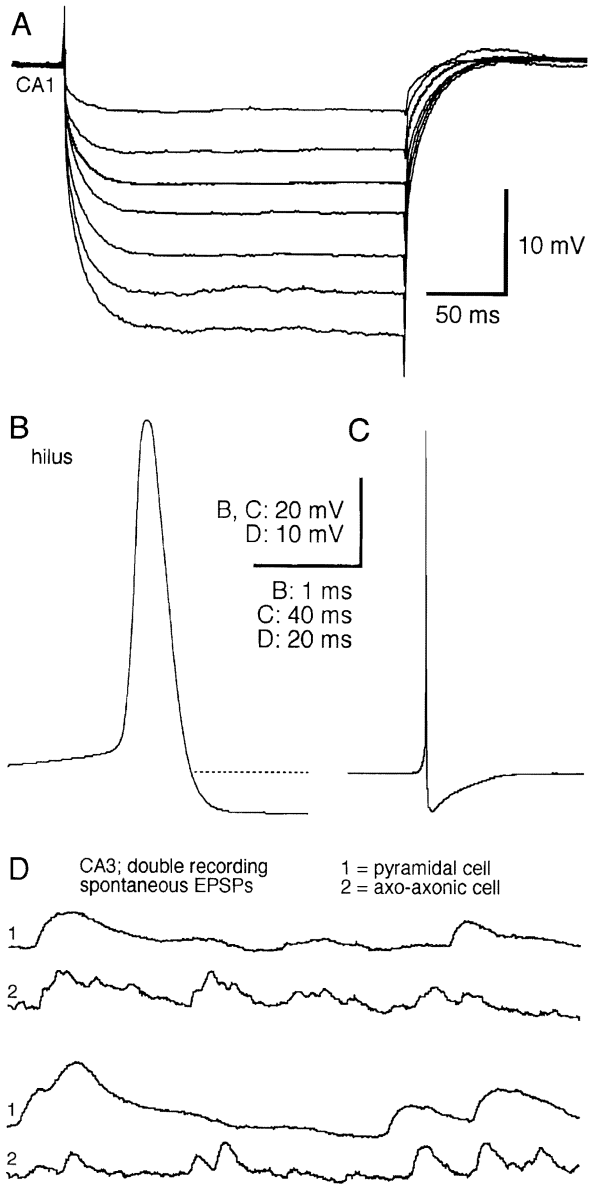

FIG. 4. *A*: current-voltage relationship of an axo-axonic cell (membrane potential −69 mV; shown in Fig. 1) in subfield CA1. Responses were superimposed after the injection of hyperpolarizing pulses in −0.1-nA increments. *B* and *C*: averaged action potentials in a hilar axo-axonic cell. Low-frequency spontaneous discharge was elicited by depolarizing the cell to firing threshold with the injection of constant depolarizing current. The cell had a short-duration action potential (0.31 ms at half-amplitude) that was followed by a deep, short-latency hyperpolarizing afterpotential (fAHP) that decayed within 31 ms back to baseline. Note the fast rate of spike repolarization and the absence of a depolarizing afterpotential. *D*: spontaneous synaptic events were simultaneously recorded from a pyramidal cell (1; membrane potential −71 mV) and an axo-axonic cell (2; membrane potential −72 mV) in the CA3 area. The excitatory postsynaptic potentials (EPSPs) in the axo-axonic cell were fractionated and appeared to be composed of a few relatively large events.

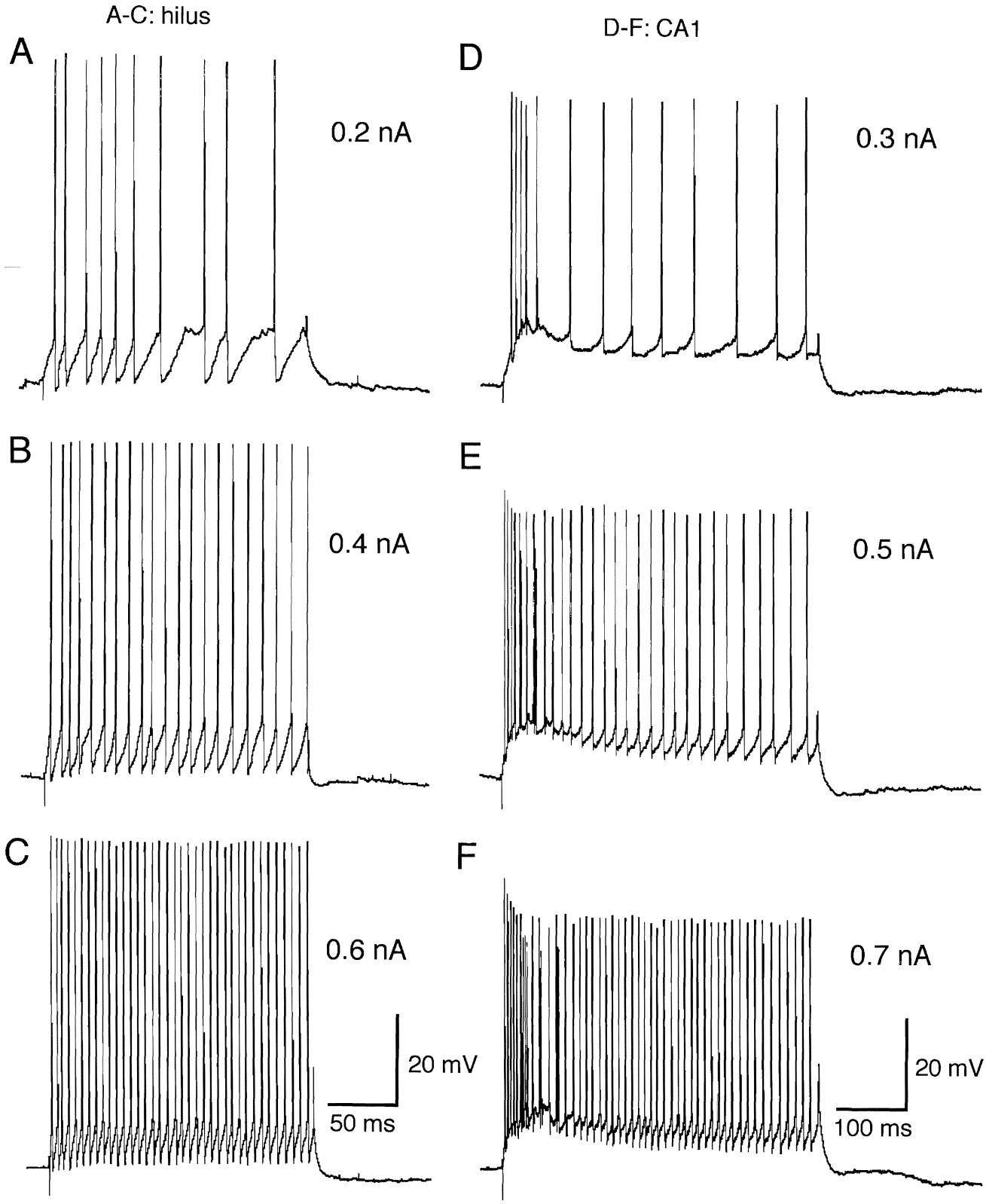

FIG. 5. Responses of 2 different axo-axonic cells to the injection of suprathreshold depolarizing current pulses. Increasing the current amplitude invariably resulted in higher firing rates. *A–C*: the majority of cells, here an example from the dentate hilus (membrane potential −64 mV), showed little spike frequency adaptation. *D* and *E*: in contrast, some axo-axonic cells, here from subfield CA1 (membrane potential −72 mV), were characterized by a marked attenuation of their firing rate. During the period of strongest adaptation the action potentials were riding on a depolarizing wave. Also note the concomitant decrease in action potential amplitude.

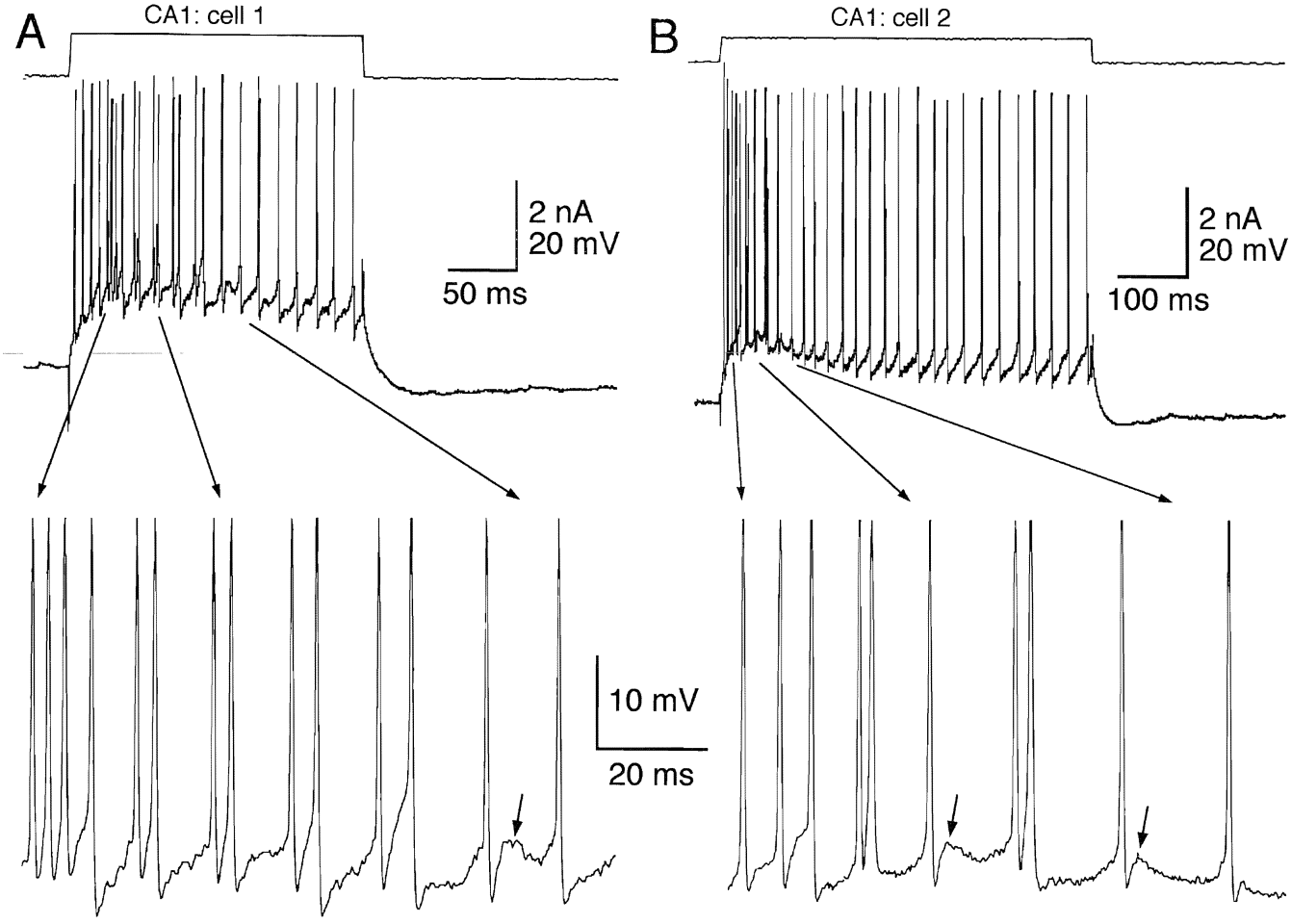

FIG. 6. *A* and *B*: 2 examples of axo-axonic cells in subfield CA1 that showed strong spike frequency accommodation and revealed an irregular firing pattern. The cell in *A* had a membrane potential of −70 mV, the cell in *B* −71 mV. During the period of strongest adaptation the cells responded with numerous doublets, i.e., an action potential followed by another with very short latency. The appearance of doublets invariably coincided with the presence of a prominent depolarizing afterpotential (short arrows) that appeared to be of sufficient amplitude to reach spike threshold frequently and thus trigger a 2nd action potential. Long arrows: *bottom panels* are expanded sections of the traces above. Note the clipping of all action potentials in the *bottom traces*. The responses in *A* are from the cell shown in Fig. 1.

CA1 (n = 4; mean adaptation of 71%) differed markedly from what is commonly observed in pyramidal or granule cells (Dudek et al. 1976; Fricke and Prince 1984; Kandel and Spencer 1961; Madison and Nicoll 1984; Staley et al. 1992). The firing pattern of these axo-axonic cells was characterized by an initial acceleration of their firing rate before they eventually started to accommodate (Fig. 5, *D–F*). This initial increase in the cell's firing rate coincided with a conspicuous depolarizing wave or hump that peaked with a latency of 29–53 ms (Fig. 5, *D–F*).

SPIKE DOUBLETS ARE TRIGGERED BY A DEPOLARIZING AFTERPOTENTIAL. During the period of marked spike frequency adaptation, several (n = 5) strongly accommodating axo-axonic cells revealed numerous spike doublets, here defined as an action potential followed by another with a relatively short latency (Fig. 6). All cells were located in subfield CA1 and in physiological terms appeared to be healthy. Their average RMP was 67.4 ± 3.6 mV, their input resistance was 56.4 ± 16.4 MΩ, and three of the cells could fire at >300 Hz. The duration of the doublet interval could range between 2.4 and 6.1 ms, with the following interspike interval being at least twice as long. Up to four distinct doublets occurred predominantly during the period of strong accommodation (Fig. 6*A*). Alternatively, several doublets could be interspersed with single action potentials (Fig. 6*B*). If so, the latter were invariably followed by a prominent depolarizing afterpotential (DAP) that had the same peak latency as the preceding doublet interval. Thus it appears that during the period of strongest spike frequency adaptation action potentials are succeeded by a prominent DAP that may or may not be of sufficient amplitude to trigger a second, short-latency discharge. During the subsequent stages of a current pulse, strongly adapting axo-axonic cells resumed a regular firing pattern because the strength of the DAP was apparently not sufficient to elicit any further doublets.

HYPERPOLARIZING AFTERPOTENTIALS. In all axo-axonic cells, current-induced action potentials were usually curtailed by a deep, short-latency hyperpolarizing afterpotential (fAHP) that appeared as a continuation of the spike repolarization (Figs. 4*C* and 5). Occasionally, e.g., after spike doublets (Fig. 6*B*), there was no apparent fAHP.

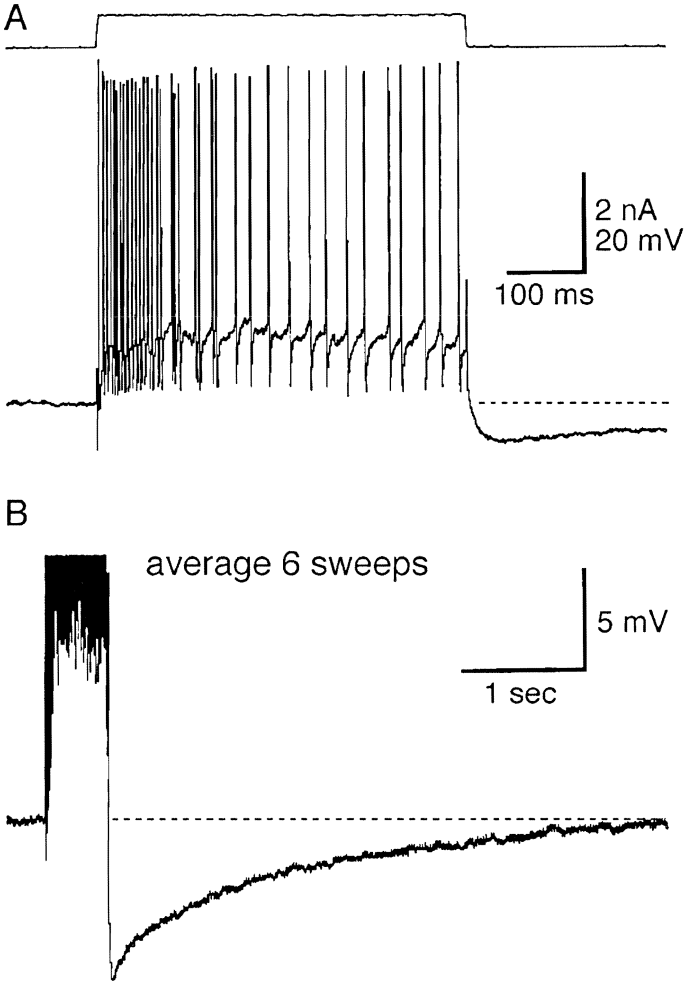

FIG. 7. *A*: in strongly adapting axo-axonic cells trains of action potentials were followed by a late afterhyperpolarizing potential (lAHP). *B*: when several depolarizing current pulses of the same duration and amplitude were averaged and displayed with both higher voltage gain and expanded time base, it is apparent that the lAHP duration may exceed a total of 4 s. The lAHP could be fitted with a single exponential with a time constant of 965 ms. Membrane potential −59 mV.

When measured from spontaneous action potentials (elicited by the injection of constant depolarizing current) the fAHP had a mean amplitude of 10.2 ± 2.8 mV and returned to baseline after 28.1 ± 12.0 ms.

A second, long-duration hyperpolarizing afterpotential (lAHP) was apparent after bursts of action potentials (Fig. 7) predominantly in cells with marked spike frequency adaptation. Such an event was observed in one dentate gyrus cell and six CA1 axo-axonic cells. Although not systematically investigated, the duration and amplitude of the lAHP were evidently correlated with both the burst duration and the total number of action potentials. The lAHP decayed fast initially before slowly approaching the baseline, suggesting an exponential decay. Therefore in three cells, one of which is illustrated in Fig. 6, several 300- to 500-ms depolarizing current pulses were averaged to reduce baseline noise and eliminate fluctuations that were due to spontaneous synaptic events. The resulting averages of the lAHP (Fig. 7*B*) were fitted with a single exponential that had a mean time constant of 1.15 ± 0.40 s.

EPSPs

For orthodromic and/or antidromic activation of afferent and efferent pathways we placed a bipolar stimulation electrode into *1*) the alveus/stratum oriens border at the subicular side of the recorded neuron, resulting in antidromic activation of CA1 pyramidal cells and the stimulation of alvear afferents, such as commissural fibers (Fig. 8*Aa*); *2*) the stratum radiatum at the CA3/CA1 junction, thus activating Schaffer collaterals (Fig. 8*Ab*); *3*) into the distinct myelinated fiber bundle that courses through the subiculum into the stratum lacunosum moleculare of the CA1 region, thus activating perforant path fibers (Fig. 8*Ac*) (Colbert and Levy 1992; Witter et al. 1988); *4*) the pyramidal cell layer of the proximal CA3 area, thus activating CA3 pyramidal cell input to the inner third of the dentate gyrus molecular layer and the hilus (Fig. 8*Ba*) (Li et al. 1994); and *5*) for hilar axo-axonic cells, into the subicular perforant path bundles that were about to cross the hippocampal fissure (Fig. 8*Bb*).

Low-intensity stimulation from all activation sites resulted in short-latency EPSPs (Fig. 8, *A*, *B*, *Ca*, and *Cb*), which could have several distinct peaks and appeared to be composed of several smaller EPSPs. With the same stimulation strength, the EPSP amplitude could fluctuate considerably. However, on average, EPSP amplitudes increased steadily with higher stimulation intensities. In the subthreshold range EPSPs were rarely contaminated by obvious IPSPs. Suprathreshold stimulation intensities normally elicited a single action potential (Fig. 8*Cc*) and only in one instance (CA1) very high stimulation intensities recruited up to three action potentials (Fig. 8*Ce*). In general, fAHPs after synaptically evoked action potentials were less conspicuous than current-evoked ones (Fig. 8, *Cc–Ce*).

EPSP PARAMETERS. Because the rather high variability of individual trials could introduce a sampling bias, postsynaptic potential measurements were only undertaken if a sufficiently smooth average at a fixed stimulation strength was available. For Schaffer collateral stimulation the average 10–90% rise time of a subthreshold EPSP was estimated to be 3.0 ± 1.1 ms, whereas the EPSP width at half-amplitude averaged 21.0 ± 1.4 ms. In dentate axo-axonic cells the EPSP resulting from CA3 stimulation had a 10–90% rise time of 5.6 ± 0.7 ms and a mean duration of 13.7 ± 2.5 ms at half-amplitude. When comparing within the same cell the shapes of EPSPs resulting from different stimulation sites, such as alvear versus Schaffer collateral stimulation in CA1 (Fig. 8*Ad*) and perforant path versus CA3 stimulation in the dentate gyrus (Fig. 8*Bc*), differences with respect to rise time and duration were apparent.

VOLTAGE DEPENDENCE OF EPSPs. We examined the voltage sensitivity of subthreshold EPSPs in four cells by averaging synaptic responses at different membrane potentials. In subfield CA1 we examined three inputs, Schaffer collaterals (Fig. 9*A*), perforant path (Fig. 9*B*), and alvear stimulation (Fig. 9*C*). Invariably the amplitude of the EPSP increased with successive hyperpolarization (Fig. 9, *A–C*). When the mean EPSP amplitude was plotted against membrane potential, there appeared to be a linear relationship. Therefore a line was fitted to the data using linear regression (Fig.

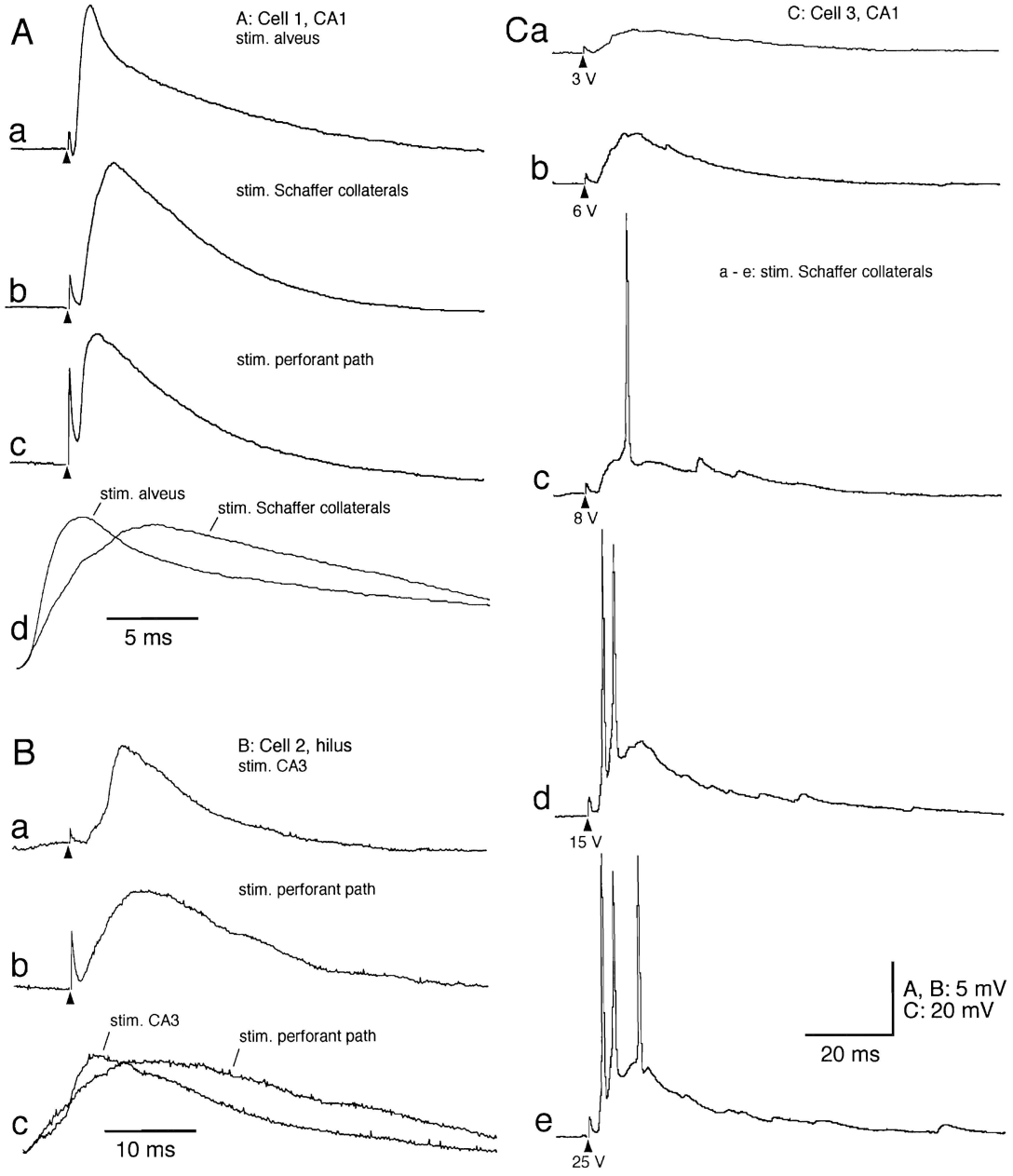

FIG. 8. Synaptic activation of axo-axonic cells. *A*: averages of subthreshold EPSPs in 1 CA1 axo-axonic cell (membrane potential −73 mV) after stimulation of 3 different activation sites, the alveus (*a*), Schaffer collaterals (*b*), and the perforant pathway (*c*). On superimposition it is apparent that the EPSP after alvear stimulation had a shorter rise time and duration when compared with the Schaffer collateral EPSP (*d*). *B*: averages of subthreshold EPSPs in a dentate axo-axonic cell (membrane potential −66 mV) after stimulation of the CA3 area (*a*) or the perforant path fiber bundles traversing the subiculum (*b*). On superimposition it is obvious that the perforant path EPSP was characterized by a markedly slower rise time and duration than the EPSP resulting from CA3 region stimulation (*c*). *C*: responses of a CA1 axo-axonic cell (membrane potential −70 mV) after stimulation of the Schaffer collateral pathway. In the subthreshold range (*a* and *b*) increasing the stimulation intensity resulted in larger EPSP amplitudes. Graded suprathreshold stimuli (*c–e*) elicited ≤3 action potentials. Moreover, stronger stimuli also decreased the latency between stimulus onset and the first action potential. Arrowheads: stimulation artifacts. Note that time base is as shown at *bottom right* except for *Ad* and *Bc*.

9*E*). In the CA1 area the extrapolated values for the EPSP reversal potential were +10.5 mV for the Schaffer collateral input and +9.3 mV for the alvear input, indicating similar underlying receptor mechanisms.

Diverging from the pattern of voltage sensitivity found in the CA1 area, the perforant path input to a dentate axo-axonic cell indicated a rather complex relationship between EPSP amplitude and membrane potential (Fig. 9, *D* and *F*). With the cell being hyperpolarized there was no obvious trend between EPSP size and membrane potential. However, close to the threshold the EPSP increased abruptly and rather markedly (Fig. 9*F*). Note that in contrast to other axo-axonic cells this particular neuron showed marked inward rectification.

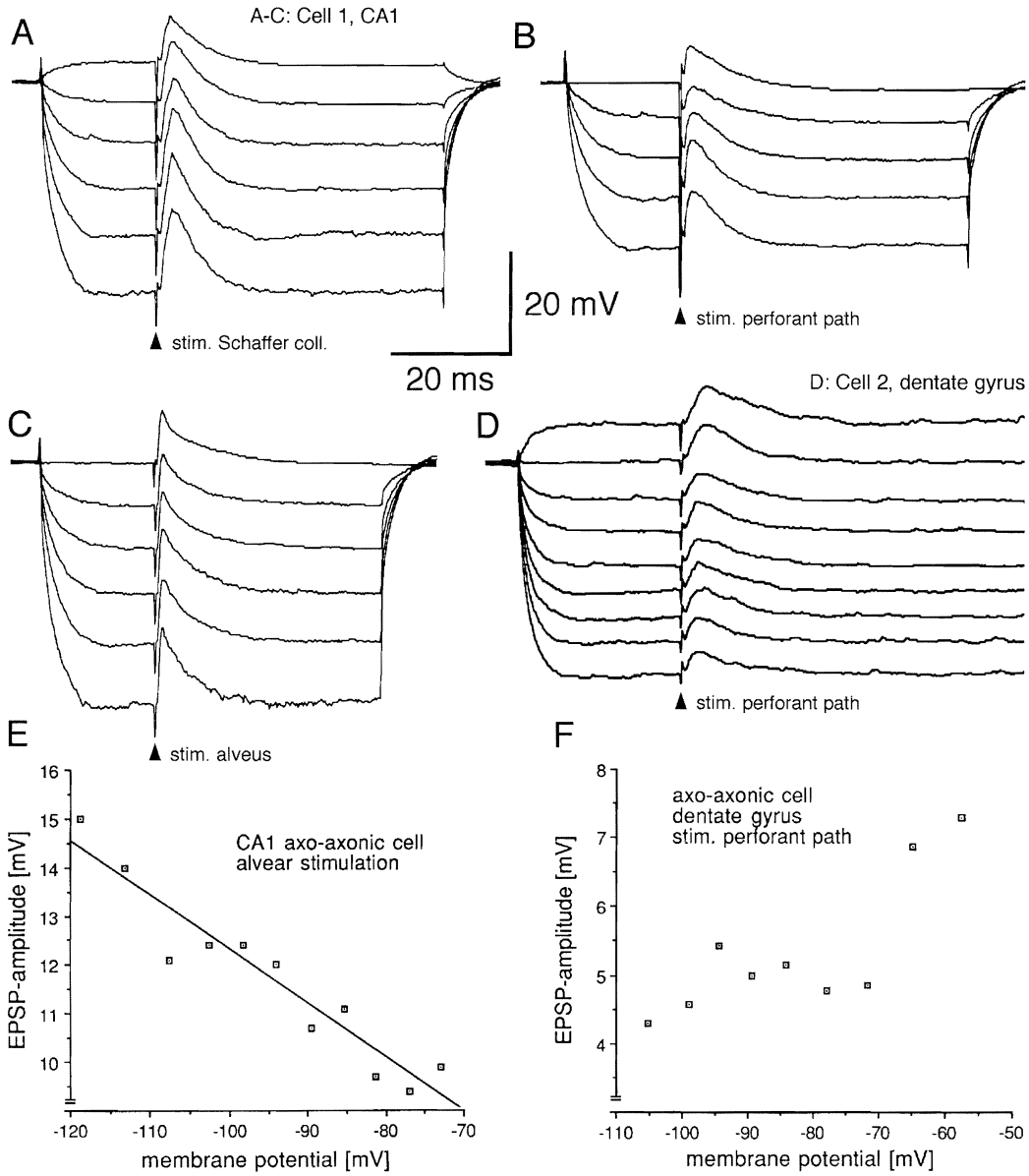

FIG. 9. Voltage sensitivity of EPSPs evoked in axo-axonic cells. In subfield CA1 (*A–C*, all traces from the same cell; membrane potential −73 mV) and the dentate gyrus (*D*; membrane potential −65 mV) the voltage dependence of subthreshold EPSPs was explored by delivering stimuli with constant strength during the concomitant injection of hyper- and depolarizing current pulses (increments of 0.2 nA in *A–C*, 0.1 nA in *D*). In all traces >3 successive events were averaged to reduce intertrial variability. In CA1 the voltage sensitivity of all EPSPs appeared to be uniform. After stimulation of 3 different inputs, the Schaffer collateral pathway (*A*), the perforant path (*B*), and the alveus (*C*), the EPSP amplitude increased with hyperpolarization. *E*: alvear EPSP amplitude appears linearly correlated with the membrane potential. With the aid of linear regression a line was fitted to the data and the EPSP was extrapolated to reverse at 9.3 mV. *D* and *F*: in the dentate gyrus the voltage sensitivity of the perforant path EPSP was more complex. Note, however, the marked increase of the EPSP amplitude at more depolarized membrane potential levels.

EXCITATORY AMINO ACID RECEPTORS. In three cells of the CA1 region stimulation of the Schaffer collaterals (Fig. 10, *A* and *B*; $n = 2$) and the alveus (Fig. 10*C*; $n = 1$) elicited subthreshold EPSPs. Interestingly the averaged Schaffer collateral EPSP in one of the cells (Fig. 10*A*) revealed two peaks, a finding that was also observed in two further axo-axonic cells. The EPSPs showed the same voltage dependence illustrated in Fig. 10, *A–C*. After the control responses had been monitored for ≥10 min and were judged to be stable, two slices were superfused with a 30-μM solution of the *N*-methyl-D-aspartate (NMDA) receptor antagonist DL-2-amino-5-phosphonopentanoic acid (AP5; Fig. 10, *B* and *C*). In the Schaffer collateral EPSP AP5 resulted in a small-amplitude increase of the early EPSP, possibly because of the elimination of a polysynaptic IPSP, and an obvious reduction of the late EPSP (Fig. 10*B*). In contrast, the alvear EPSP in a different axo-axonic cell was unaffected by AP5 application (Fig 10, *Ca–Cc*). Subsequently, in the same cell, an additional 5 μM of the non-NMDA excitatory amino acid antagonist 6-cyano-7-nitroquinoxaline-2,3-dione (CNQX; Honore et al. 1988) was added to the superfusate, resulting in a dramatic reduction of the

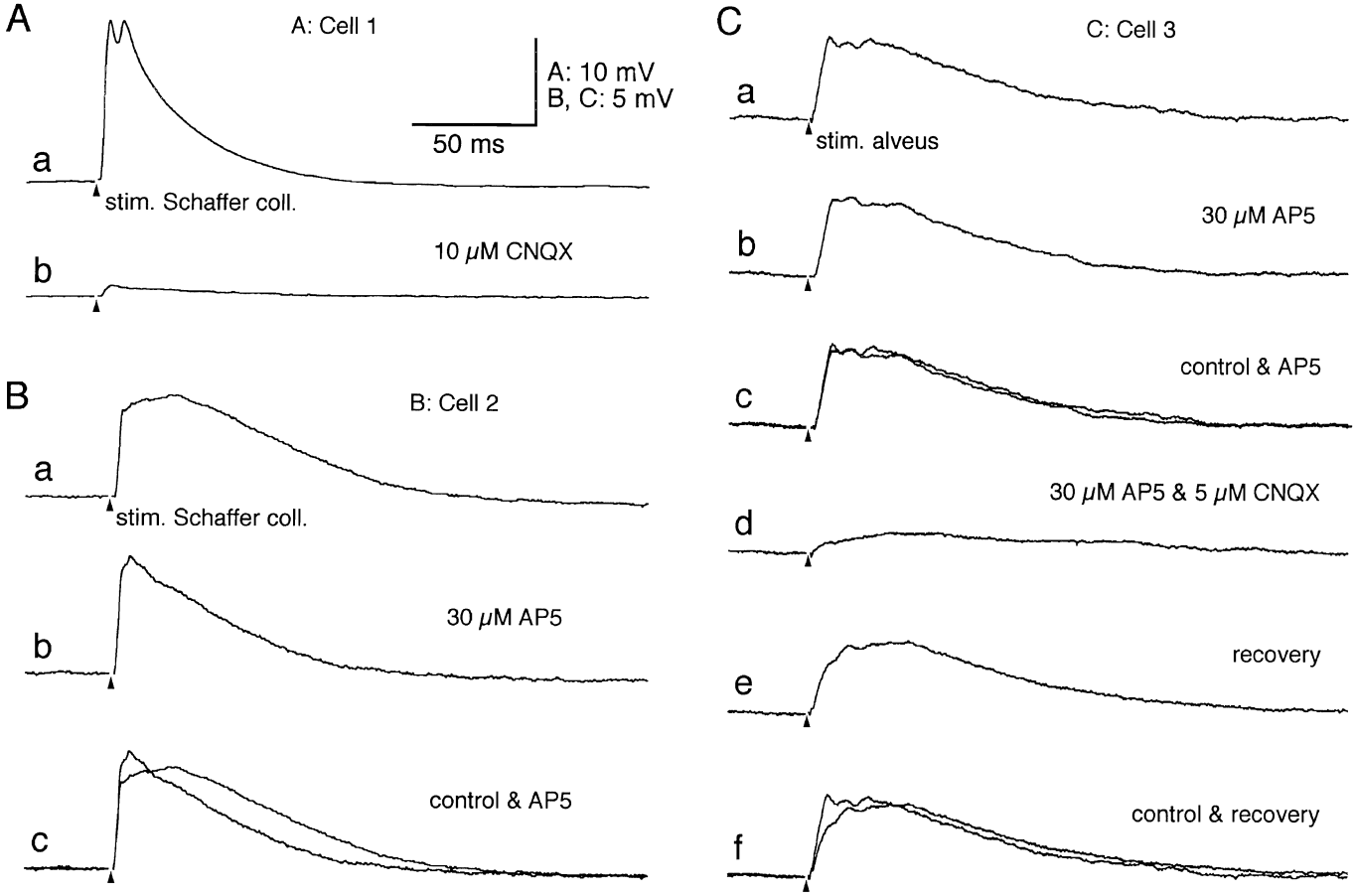

FIG. 10. Sensitivity of EPSPs evoked in 3 CA1 axo-axonic cells to bath-application of glutamate receptor antagonists. All traces are averages of >10 responses to avoid intertrial variability. *Aa*: control EPSP evoked by Schaffer collateral stimulation at −69 mV membrane potential. Same cell as in Fig. 1. *Ab*: superfusion with 10 μM 6-cyano-7-nitroquinoxaline-2,3-dione (CNQX) reduced the amplitude of the control response by 96%. *Ba*: in a 2nd cell (−66 mV membrane potential) bath-application of 30 μM DL-2-amino-5-phosphonopentanoic acid (AP5) decreased the late phase of the Schaffer collateral control EPSP (*Bb* and *Bc*). Interestingly, the early phase of the EPSP showed a small amplitude increase that may be due to the reduction of a shunting polysynaptic inhibitory postsynaptic potential (IPSP). *Ca–Cc*: in a 3rd axo-axonic cell (-64 mV membrane potential) superfusion of 30 μM AP5 had no effect on the alvear control EPSP, whereas an additional 5 μM CNQX in the superfusate resulted in a 75% reduction of the EPSP amplitude. *Ce* and *Cf*: after return to control ACSF the EPSP showed almost complete recovery. Arrowheads: stimulation artifacts, which have been removed for clarity.

EPSP amplitude (Fig. 10 *Cb–Cd*). At a higher concentration (10 μM), CNQX was effective in almost obliterating the Schaffer collateral EPSP in a different cell (Fig. 10*A*). In one instance (Fig. 10, *Ce* and *Cf*) almost complete recovery of the control EPSP was achieved after perfusion with normal ACSF. In the two remaining cells concomitant monitoring of input resistance and time constant showed no changes during the period of drug application.

IPSPs

When activating any of the major afferent pathways, subthreshold stimulus intensities generally failed to elicit IPSPs >1 mV in amplitude. Large-amplitude IPSPs were only recruited when the stimulus strength was adjusted to approximately twice the spike threshold. IPSPs were composed of an early $IPSP_A$ that peaked at 28.9 ± 5.0 ms latency (Fig. 11, *A* and *C*), to be followed by a late $IPSP_B$ (mean duration 671 ± 37 ms) that attained its maximum at a mean latency of 124.8 ± 6.4 ms (Fig. 11*B*). Both components were readily distinguishable by varying the membrane potential. The early $IPSP_A$ began to reverse at a mean membrane potential of −66.5 ± 3.3 mV and further hyperpolarization resulted in response reversal (Fig. 11*A*). In contrast, the late $IPSP_B$ was still present at membrane potentials more negative than −70 mV. Its precise reversal was generally difficult to determine because during hyperpolarization its early phase became occluded by the predominant depolarizing $IPSP_A$.

The efficacy of the IPSP was determined by delivering a strong stimulus to an afferent pathway during depolarization-induced repetitive firing (Fig. 11*C*). A control response with the same current intensity is also illustrated to demonstrate that the hyperpolarization seen in Fig. 11*C* was not due to a prominent AHP after the cell's rapid initial discharge (Fig. 11*D*). In the second half of the 200-ms control response the CA1 cell was firing at a mean frequency of 46 Hz (Fig. 11*D*). During the successive current pulse the Schaffer collateral input was activated with a single shock at twice the spike threshold intensity (Fig. 11*C*). The resulting IPSP was effective in completely suppressing depolarization-induced firing for the remainder of the pulse (117 ms).

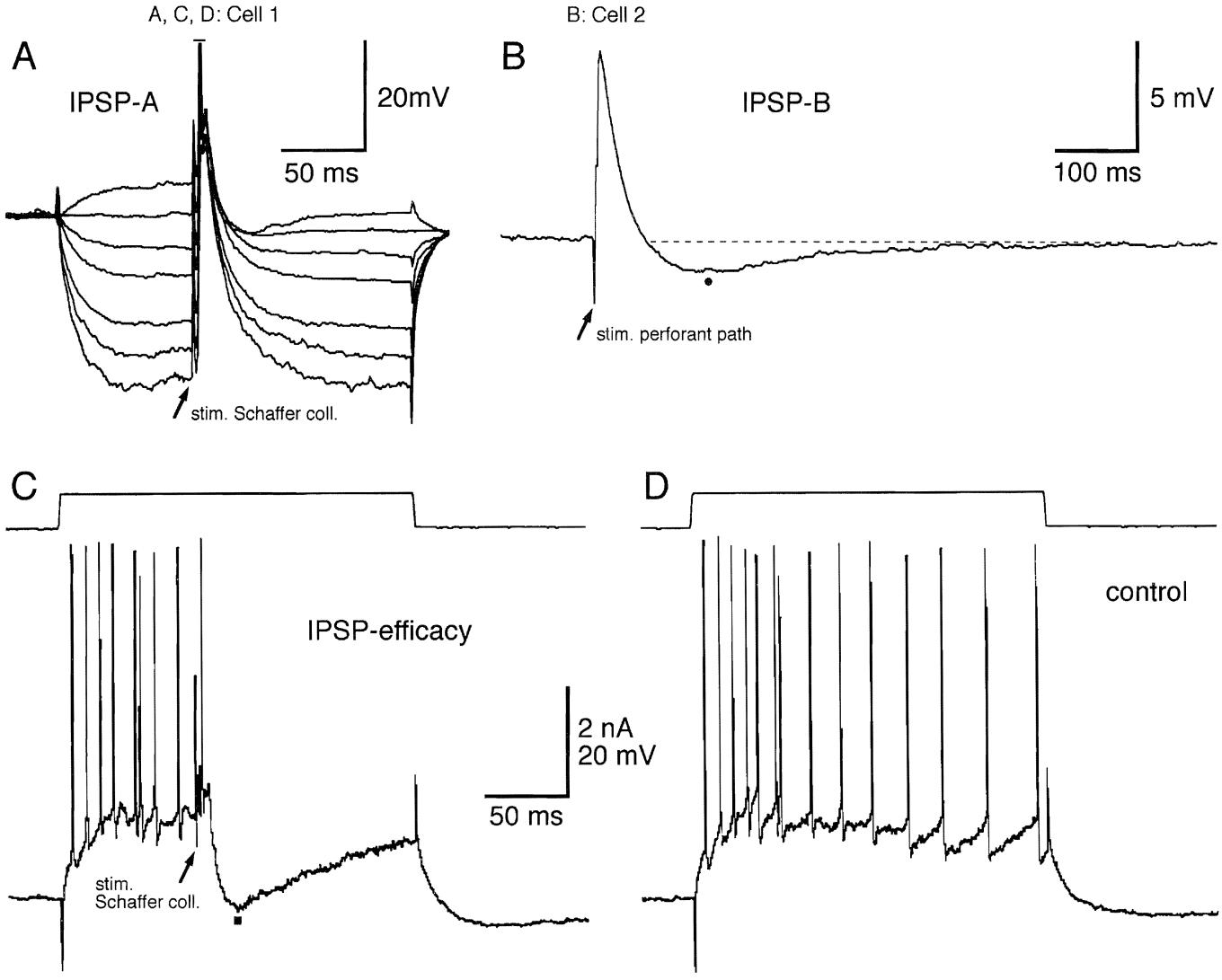

FIG. 11. Strong synaptic stimuli (↑) elicited an EPSP/IPSP sequence in 2 axo-axonic cells, here in subfield CA1, in response to Schaffer collateral (*A* and *C*) or perforant path (*B*) stimulation. IPSPs were composed of 2 components, (*A*) an early $IPSP_A$ with a mean reversal potential of −66.5 mV and (*B*) a late $IPSP_B$ (●; membrane potential −68 mV) with an average duration of 671 ms. *C*: efficacy of the early IPSP (■) in preventing CA1 axo-axonic cells from firing was determined by delivering a strong synaptic stimulus to the Schaffer collaterals concomitant with a suprathreshold depolarizing current pulse. The resulting IPSP was effective in completely suppressing depolarization-induced firing for the remainder of the current pulse. *D*: control response to the same amplitude current injection but without synaptic stimulation. The traces in *A*, *C*, and *D* are from the cell illustrated in Fig. 1. Membrane potential −67 mV.

DISCUSSION

Employing intracellular recording techniques and subsequent filling with the marker biocytin it was feasible to characterize physiologically a population of GABAergic hippocampal interneurons, the axo-axonic cells, which are morphologically homogeneous with respect to their efferent connectivity. This approach was taken because several previous studies already indicated that hippocampal interneurons in different layers were not only diverse in their physiological properties (Kawaguchi and Hama 1987, 1988; Lacaille and Schwartzkroin 1988a; Lacaille and Williams 1990) but may also differ in their postsynaptic effects on the respective principal cell population (Lacaille et al. 1987; Lacaille and Schwartzkroin 1988b; Miles 1990; Miles and Wong 1984).

Anatomic properties of identified axo-axonic cells

Employing the Golgi-impregnation method and intracellular filling techniques axo-axonic cells were previously encountered in subfield CA1 and the dentate gyrus of the mammalian hippocampus (Halasy and Somogyi 1993; Han et al. 1993; Kosaka 1980, 1983; Li et al. 1992; Somogyi et al. 1983, 1985; Soriano and Frotscher 1989; Soriano et al. 1990). From these studies it emerged that axo-axonic cells constitute a unique type of hippocampal local circuit cell with its output strictly confined to the initial segment of their respective postsynaptic target cells. In this study their highly distinctive light microscopic features enabled the morphological identification of a total of 17 axo-axonic cells that were encountered in all hippocampal subfields. Whenever used, electron microscopy confirmed the

correctness of the light microscopic assessment. Labeled terminals invariably established their synapses only with the initial segment of their respective target cells even when the initial segments were outside their normal layer, e.g., in the stratum radiatum. Finally, in agreement with previous results (Somogyi et al. 1985), the GABAergic nature of axo-axonic cells was ascertained using antibodies directed against GABA and a highly sensitive immunogold-silver intensification procedure (Halasy and Somogyi 1993).

The anatomic observations presented above largely confirm those of previous studies (Halasy and Somogyi 1993; Han et al. 1993; Li et al. 1992; Somogyi et al. 1983, 1985; Soriano and Frotscher 1989; Soriano et al. 1990). Two findings, however, appear to be noteworthy. First, all hilar axo-axonic cells and, surprisingly, even one neuron that was clearly positioned in the pyramidal cell layer of subfield CA3 (CA3c) had several of their dendrites penetrating the granule cell layer and ascending into the dentate molecular layer. This observation corroborates our physiological data showing short-latency synaptic activation of hilar axo-axonic cells after stimulation of perforant path fibers. Thus it appears that hilar axo-axonic cells may receive direct entorhinal input. Likewise, all axo-axonic cells in the CA1 area had extensive dendritic tufts in the stratum lacunosum moleculare, which is also targeted by a substantial entorhinal projection (Witter et al. 1988). Second, light microscopic estimates indicated that a CA1 axo-axonic cell in a 400-μm slice may contact as many as 686 pyramidal cells. When compared with the number of postsynaptic targets of an axo-axonic cell that was filled under in vivo conditions and reconstructed from the whole brain (n = 1,214; Li et al. 1992) it appears that about half of the cell's total axonal arbor may be contained in a 400-μm-thick slice preparation. Therefore a substantial part of the functional circuits involving axo-axonic cells may be preserved in conventional slice preparations.

Comparative electrophysiology: axo-axonic and principal cells

Our results clearly show that axo-axonic cells have distinct membrane and firing properties that allow them to be unambiguously discriminated from the prevalent principal cell types, such as the pyramidal cells of the Ammon's horn or granule and mossy cells of the dentate gyrus. All cells had relatively short time constants and fast, nonovershooting action potentials that were usually followed by a deep fAHP, properties in which they differ markedly from principal neurons (Brown et al. 1981; Fricke and Prince 1984; Scharfman 1992; Scharfman et al. 1990; Spencer and Kandel 1961; Storm 1987; Wong and Prince 1981). Other distinguishing properties, most notably spike frequency adaptation and the presence of afterpotentials, such as DAPs and lAHPs, were of lesser discriminatory value. Although generally present in principal cells of the hippocampus (for review see Schwartzkroin and Mueller 1987) these features were also found in a minor proportion of axo-axonic cells.

Comparative electrophysiology: interneurons

In many of their membrane and firing properties axo-axonic cells were similar to those previously reported for interneurons in the stratum oriens and pyramidal layer of the CA1 area (Ashwood et al. 1984; Kawaguchi and Hama 1988; Lacaille 1991; Lacaille and Williams 1990; Lacaille et al. 1987; Schwartzkroin and Mathers 1978), in the dentate gyrus (Misgeld and Frotscher 1986; Scharfman 1991; Scharfman and Schwartzkroin 1990; Scharfman et al. 1990), and in cortical interneurons (Connors and Gutnick 1990; McCormick et al. 1985). When comparing these data it appears that interneurons in these cortical regions share several properties, such as a short time constant or a short-duration action potential that is mainly due to the very rapid rate of fall of the action potential (McCormick et al. 1985), presumably mediated by particularly strong repolarizing potassium currents (Hamill et al. 1991; Scharfman 1991). The latter notion would also explain our finding and those of previous studies showing that interneurons may have relatively small-amplitude, barely overshooting action potentials (Ashwood et al. 1984; Lacaille et al. 1987, 1989; Schwartzkroin and Kunkel 1985; Schwartzkroin and Mathers 1978). Likewise, the same potassium conductance that appears to "clip" the action potentials may be also responsible for the large-amplitude fAHP, which is a very consistent feature of most hippocampal and neocortical interneurons (Lacaille and Williams 1990; McCormick et al. 1985; Misgeld and Frotscher 1986; Schwartzkroin and Mathers 1978).

Differences between interneuron properties are evident when comparing such parameters as RMP, input resistance, and the rate of spontaneous firing. Many of these measurements may, however, not reflect intrinsic properties of the cells but rather the quality of impalement or other extraneous factors, such as the temperature and composition of the ACSF. In this respect it is interesting to note how, for example, the parameters that have been reported for dentate granule cells differ between individual studies (compiled in Lambert and Jones 1990).

Apart from these rather variable factors, a number of other parameters appear to discriminate local circuit cells of the molecular layer (Kawaguchi and Hama 1987, 1988; Lacaille and Schwartzkroin 1988a) from axo-axonic cells. The former are characterized by relatively long-duration action potentials CA1 half-amplitude 0.61 ms (Kawaguchi and Hama 1988) vs. 0.39 ms for axo-axonic cells], they display anodal break excitation and may fire bursts of action potentials in response to membrane hyperpolarization (Lacaille and Schwartzkroin 1988a). In this respect axo-axonic cells resemble more closely interneurons of the pyramidal cell layer (Ashwood et al. 1984; Kawaguchi and Hama 1988; Lacaille 1991; Schwartzkroin and Mathers 1978), although this similarity may partially reflect the fact that axo-axonic cells constitute a substantial proportion of this morphologically heterogeneous population (Buhl et al. 1993).

In most of their intrinsic properties axo-axonic cells were also similar to the population of stratum oriens-alveus interneurons of the CA1 region (Lacaille et al. 1987; Lacaille and Williams 1990); for example, all cells show a certain degree of spike frequency adaptation. However, despite their overall similarity, stratum oriens-alveus interneurons have a substantially longer action potential (0.55 ms at half-amplitude) and show a marked degree of time-dependent inward rectification as well as anodal break excitation

(Lacaille and Williams 1990). It remains to be determined whether these differences in the intrinsic properties of interneurons reflect their electrical geometry, a differential distribution or density of channels, or possibly a different composition of channels. In this respect it is interesting to note that when comparing neocortical pyramidal and stellate cells (the latter presumed to be largely GABAergic local circuit cells), both all-or-none as well as quantitative differences in the expression of channels may exist (Hamill et al. 1991).

Variability of physiological properties

As yet there is no anatomic evidence indicating that axo-axonic cells are heterogeneous in their connections. On the contrary, all available data suggest that axo-axonic cells are an example of a stereotyped population of local circuit cells. However, in vitro they were found to be surprisingly diverse in several of their intrinsic physiological properties, namely the degree of spike frequency adaptation, the variable expression of a DAP, appearing in conjunction with spike doublets and, finally, the presence or absence of a marked lAHP.

One possible explanation for this physiological diversity would be that axo-axonic cells constitute a heterogeneous class of cells. Although this finding is difficult to reconcile with the anatomic data, an alternative but equally simple explanation is that axo-axonic cells in vitro may show functionally different states of activity similar to hippocampal lacunosum moleculare interneurons that can change their mode of firing from "sustained" to "burst" in response to membrane hyperpolarization (Lacaille and Schwartzkroin 1988a). In thalamic neurons this transition between discharge modes is attributable to a low-threshold voltage-dependent calcium conductance (reviewed in Llinas 1988), which is also present in lacunosum moleculare interneurons (Fraser and MacVicar 1991). The presence or absence of such a conductance in axo-axonic cells remains to be tested. The spike frequency accommodation that follows an initial acceleration of the firing rate may be due to the activation of a calcium-dependent potassium current (Madison and Nicoll 1984; Storm 1987, 1990). Such a conductance may also be responsible for the concomitant generation of a long-lasting AHP that could follow depolarizing current pulses (Hotson and Prince 1980; Lancaster and Adams 1986). In cortical and hippocampal pyramidal cells calcium influx has been also implicated in the generation of DAPs, which in turn may promote the occurrence of spike doublets and initiate burstiness (Connors et al. 1982; Costa et al. 1991; Friedman and Gutnick 1989; Wong and Prince 1978).

Synaptic excitation of axo-axonic cells

Whenever tested, axo-axonic cells invariably responded with a short-latency EPSP after stimulation of afferent pathways. Thus a monosynaptic activation of axo-axonic cells by hippocampal afferents appears likely. They may therefore participate in feedforward inhibition of the principal cell population, as has been repeatedly proposed for hippocampal interneurons that were identified on morphological and/or physiological grounds (Ashwood et al. 1984; Buzsaki 1984; Frotscher 1991; Frotscher and Zimmer 1983; Lacaille 1991; Scharfman 1991; Taube and Schwarzkroin 1987). Consistent low-threshold activation by pathways with spatially restricted termination fields is corroborated by the finding that axo-axonic cells extended their dendrites throughout all hippocampal layers. It appears, therefore, that axo-axonic cells may integrate inputs from a broad range of hippocampal afferents. Moreover, axo-axonic cells in the CA1 area had many of their basal dendrites within the lower stratum oriens and neighboring alveus, where the recurrent collaterals of principal cells form a dense plexus. This suggests that axo-axonic cells may also participate in feedback circuits. This notion is of functional relevance because the dendritic geometry of other hippocampal local circuit cells presumably reflects the spatially restricted availability of their inputs (Han et al. 1993).

It is also noteworthy that stimulation of the CA3 area activated hilar axo-axonic cells that, in turn, innervate dentate granule cells. Thus a possible recurrent input from CA3 pyramidal cells may reduce granule cell activity and their mossy fiber output to the CA3 area. The anatomic basis for such a recurrent circuit was recently established by Li et al. (1994) who showed that CA3c pyramidal cells provide a significant input to the inner third of the molecular layer as well as the hilus of the rat dentate gyrus.

The examination of the voltage dependence of EPSPs that were elicited in axo-axonic cells rendered mixed results, which may reflect an intrinsic diversity of response properties. In axo-axonic cells of the CA1 area the EPSP amplitude steadily increased with membrane hyperpolarization. In the absence of inwardly rectifying conductances this behavior would be consistent with the response being largely mediated by the excitatory amino acid glutamate, acting on non-NMDA receptors (Jones and Baughman 1988; Sutor and Hablitz 1989a,b). And indeed bath-application of the NMDA glutamate receptor antagonist AP5 in two CA1 axoaxonic cells left the amplitude of the control EPSPs unaffected, whereas the non-NMDA receptor antagonist CNQX resulted in a prominent reduction of the test response in two instances. Thus axo-axonic cells appear to resemble principal cells of the hippocampus, where EPSPs of the major afferent pathways appear to be predominantly due to the activation of non-NMDA-type excitatory amino acid receptors (Andreasen et al. 1989; Davies and Collingridge 1989; Lambert and Jones 1990; for review see Nicoll et al. 1990). However, despite the apparent predominance of non-NMDA receptor-mediated glutamatergic neurotransmission, it is noteworthy that application of the NMDA receptor antagonist AP5 in one of the cells was effective in reducing the late phase of the control EPSP. It is possible, therefore, that in normal medium NMDA receptors may be also involved in the generation of EPSPs in axo-axonic cells. Therefore axo-axonic cells resemble other CA1 interneurons in strata oriens and radiatum, which show a variable contribution of both types of glutamate receptor, with some cells apparently lacking a demonstrable NMDA component (Sah et al. 1990).

Deviating from the pattern observed in CA1, the EPSP in an axo-axonic cell of the dentate gyrus showed a very different type of voltage dependence. Most notably, the ampli-

tude of the test response increased markedly in the subthreshold region. This behavior may reflect either the voltage-dependent recruitment of NMDA receptors (reviewed in Mayer and Westbrook 1987), the contribution of a noninactivating voltage-dependent sodium conductance, the activation of low-threshold calcium channels, or, possibly, a mixture of the above mechanisms (Deisz et al. 1991; Staffstrom et al. 1985; Sutor and Hablitz 1989a,b).

Inhibitory control of axo-axonic cells

Strong, usually suprathreshold stimuli elicited IPSPs in axo-axonic cells. Their efficacy was demonstrated by revealing their ability to suppress depolarization-induced firing. Thus a feedforward and/or recurrent IPSP may explain why axo-axonic cells never responded with more than three action potentials after synaptic activation. This notion is supported by the finding that pharmacological removal of inhibition may increase the synaptic excitability of interneurons and uncover their ability to fire rapid bursts of synaptically evoked action potentials (Lacaille 1991; Misgeld and Frotscher 1986).

Axo-axonic cell IPSPs had two components. A short-latency component of the IPSP reversed at −66.5 mV and may thus correspond to the chloride-mediated IPSP involving the activation of $GABA_A$ receptors in principal cells (Alger and Nicoll 1982a,b; for review see Nicoll et al. 1990). A similar component has been pharmacologically isolated in interneurons of the guinea pig dentate gyrus and subfield CA1 of the rat hippocampus (Lacaille 1991; Misgeld and Frotscher 1986). The IPSPs of axo-axonic cells also exhibited a late component that in its characteristics resembled the potassium-mediated IPSP that is due to the action of $GABA_B$ receptors (Newberry and Nicoll 1984, 1985; reviewed by Ogata 1990). In several instances late IPSPs have been demonstrated in hippocampal interneurons (Ashwood et al. 1984; Kawaguchi and Hama 1988; Madison and Nicoll 1988; Misgeld et al. 1989; Schwartzkroin and Mathers 1978) and their pharmacological modulation by $GABA_B$ receptor antagonists was recently shown for pyramidal cell layer interneurons in area CA1 of the rat hippocampus (Lacaille 1991). Therefore axo-axonic cells correspond to the picture emerging from the analysis of other, as yet less well-defined interneurons. It thus appears that axoaxonic cells receive GABAergic synapses that have pharmacological characteristics that resemble those of the principal cell population.

Concluding remarks

It has been suggested that the relative paucity of subthreshold currents in nonprincipal cells would be consistent with their role being largely the reliable, wide-band transformation of excitatory input into inhibitory output, with little need for modulation (Connors and Gutnick 1990; Hamill et al. 1991). Although this may be true for some "fast-spiking" cells, this somewhat simplified concept may need to be revised. It is becoming increasingly evident that interneurons from different hippocampal layers may vary in their physiological properties (Kawaguchi and Hama 1987, 1988; Lacaille 1991; Lacaille and Schwartzkroin 1988a; Lacaille and Williams 1990; Scharfman 1991). Moreover, data presented above have demonstrated that anatomically identified axo-axonic cells had firing properties (e.g., DAPs and spike doublets) that were generally assumed to be a characteristic of principal cells (e.g., Lacaille and Williams 1990). The reason why DAPs in particular have not been described for interneurons may well be because of the fact that in the absence of anatomic verification such recordings were classified as originating from principal cell types. Finally, axo-axonic cells may serve as an example to demonstrate that even a morphologically homogeneous class of local circuit cell may be surprisingly diverse in its properties under in vitro conditions. Further studies will explore the postsynaptic effect of this unique type of cortical cell.

The authors are grateful to P. Jays and F. D. Kennedy for photographic help, to L. Lyford and P. M. Twynam for secretarial assistance, and K. Boczko, D. Latawiec, and J. D. B. Roberts for excellent technical support. We thank our colleagues T. C. Cunnane, R. Douglas, K. Halasy, R. S. G. Jones, A. Mason, H. E. Scharfman, and A. Thomson for technical advice and critical discussions throughout the completion of the study. U. Heinemann kindly provided us with a model of his interface chamber.

Present addresses: Z.-S. Han, Dept. of Neurobiology, Barrow Neurological Institute, 350 West Thomas Rd., Phoenix, AZ 85013; V. V. Stezhka, University of Birmingham, Dept. of Physiology, Edgbaston, Birmingham B15 2TT, UK.

Address for reprint requests: E. H. Buhl, Medical Research Council, Anatomical Neuropharmacology Unit, Oxford University, Mansfield Rd., Oxford OX1 3TH, UK.

Received 22 February 1993; accepted in final form 29 October 1993.

NOTE ADDED IN PROOF

Since the acceptance of this paper, electron microscopic examination of a new set of interneurons has revealed cells that, in contrast to axo-axonic cells examined in this study, give synapses to both the axon initial segments and the somatodendritic region of pyramidal cells. Therefore 185 synaptic targets, with no less than 10 synapses for each axo-axonic cell reported in this study, have been re-examined. Thirteen of these cells made synapses only with axon initial segments, two of them made 1, one of them made 2 synapses with somata, thus having a preference of >90% for initial segments. One cell from the CA3 region, which is illustrated in Fig. 4*D*, made 40% of its synapses with initial segments, the remainder with dentrites and somata.

REFERENCES

AGHAJANIAN, G. K. AND RASMUSSEN, K. Intracellular studies in the facial nucleus illustrating a simple new method for obtaining viable motoneurons in adult rat brain slices. *Synapse* 3: 331–338, 1989.

ALGER, B. E. AND NICOLL, R. A. Feed-forward dendritic inhibition in rat hippocampal pyramidal cells studied in vitro. *J. Physiol. Lond.* 328: 105–123, 1982a.

ALGER, B. E. AND NICOLL, R. A. Pharmacological evidence for two kinds of GABA receptor on rat hippocampal pyramidal cells studied in vitro. *J. Physiol. Lond.* 328: 125–141, 1982b.

ANDREASEN, M., LAMBERT, J. D. C., AND JENSEN, M. S. Effects of new non-*N*-methyl-D-aspartate antagonists on synaptic transmission in the in vitro rat hippocampus. *J. Physiol. Lond.* 414: 317–336, 1989.

ASHWOOD, T. J., LANCASTER, B., AND WHEAL, H. V. In vivo and in vitro studies on putative interneurones in the rat hippocampus: possible mediators of feed-forward inhibition. *Brain Res.* 293: 279–291, 1984.

BROWN, T. H., FRICKE, R. A., AND PERKEL, D. H. Passive electrical constants in three classes of hippocampal neurons. *J. Neurophysiol.* 46: 812–827, 1981.

BUHL, E.H. Intracellular Lucifer yellow injection in fixed brain slices. In: *Experimental Neuroanatomy: a Practical Approach,* edited by J. P. Bolam. Oxford, UK: Oxford Univ. Press, 1992, p. 187–212.

BUHL, E. H., HALASY, K., AND SOMOGYI, P. Hippocampal unitary IPSPs:

identified sources and number of release sites (Abstract). *Eur. J. Neurosci.* S6: 225, 1993.

BUHL, E. H., HAN, Z. S., LÖRINCZI, Z., AND SOMOGYI, P. Physiological properties of anatomically identified axo-axonic cells in the rat hippocampus in vitro. *Soc. Neurosci. Abstr.* 22: 386, 1992.

BUZSAKI, G. Feed-forward inhibition in the hippocampal formation. *Prog. Neurobiol.* 22: 131–153, 1984.

COLBERT, C. M. AND LEVY, W. B. Electrophysiological and pharmacological characterization of perforant path synapses in CA1: mediation by glutamate receptors. *J. Neurophysiol.* 68: 1–8, 1992.

CONNORS, B. W. AND GUTNICK, M. J. Intrinsic firing patterns of diverse neocortical neurons. *Trends Neurosci.* 13: 99–104, 1990.

CONNORS, B. W., GUTNICK, M. J., AND PRINCE, D. A. Electrophysiological properties of neocortical neurons in vitro. *J. Neurophysiol.* 48: 1302–1320, 1982.

COSTA, P. F., RIBEIRO, M. A., AND SANTOS, A. I. Afterpotential characteristics and firing patterns in maturing rat hippocampal CA1 neurones in in vitro slices. *Dev. Brain. Res.* 62: 263–272, 1991.

DAVIES, S. N. AND COLLINGRIDGE, G. L. Role of excitatory amino acid receptors in synaptic transmission in area CA1 of rat hippocampus. *Proc. R. Soc. Lond B Biol. Sci.* 236: 373–384, 1989.

DEISZ, R. A., FORTIN, G., AND ZIEGLGÄNSBERGER, W. Voltage dependence of excitatory postsynaptic potentials of rat neocortical neurons. *J. Neurophysiol.* 65: 371–382, 1991.

DOUGLAS, R. J. AND MARTIN, K. A. C. Control of neuronal output by inhibition at the axon initial segment. *Neural Comp.* 2: 283–292, 1990.

DUDEK, F. E., DEADWYLER, S. A., COTMAN, C. W., AND LYNCH, G. Intracellular responses from granule cell layer in slices of rat hippocampus: perforant path synapse. *J. Neurophysiol.* 39: 384–393, 1976.

FAIREN, A. AND VALVERDE, F. A specialised type of neuron in the visual cortex of cat: a Golgi and electron microscope study of chandelier cells. *J. Comp. Neurol.* 194: 761–779, 1980.

FRASER, D. D. AND MACVICAR, B. A. Low-threshold transient calcium current in rat hippocampal lacunosum-moleculare interneurons: kinetics and modulation by neurotransmitters. *J. Neurosci.* 11: 2812–2820, 1991.

FREUND, T. F., MARTIN, K. A. C., SMITH, A. D., AND SOMOGYI, P. Glutamate decarboxylase-immunoreactive terminals of Golgi-impregnated axoaxonic cells and of presumed basket cells in synaptic contact with pyramidal neurons of the cat's visual cortex. *J. Comp. Neurol.* 221: 263–278, 1983.

FRICKE, R. A. AND PRINCE, D. A. Electrophysiology of dentate gyrus granule cells. *J. Neurophysiol.* 51: 195–209, 1984.

FRIEDMAN, A. AND GUTNICK, M. J. Intracellular calcium and control of burst generation in neurons of guinea-pig neocortex in vitro. *Eur. J. Neurosci.* 1: 374–381, 1989.

FROTSCHER, M. Target cell specificity of synaptic connections in the hippocampus. *Hippocampus* 1: 123–130, 1991.

FROTSCHER, M. AND ZIMMER, J. Commissural fibers terminate on nonpyramidal neurons in the guinea pig hippocampus—a combined Golgi/EM degeneration study. *Brain Res.* 265: 289–293, 1983.

HALASY, K. AND SOMOGYI, P. Subdivisions in the multiple GABAergic innervation of granule cells in the dentate gyrus of the rat hippocampus. *Eur. J. Neurosci.* 5: 411–429, 1993.

HAMILL, O. P., HUGUENARD, J. R., AND PRINCE, D. A. Patch-clamp studies of voltage-gated currents in identified neurons of the rat cerebral cortex. *Cerebral Cortex* 1: 48–61, 1991.

HAN, Z. S., BUHL, E. H., LÖRINCZI, Z., AND SOMOGYI, P. A high degree of spatial selectivity in the axonal and dendritic domains of physiologically identified local-circuit neurones in the dentate gyrus of the rat hippocampus. *Eur. J. Neurosci.* 5: 395–410, 1993.

HONORE, T., DAVIES, S. N., DREJER, J., FLETCHER, E. J., JACOBSEN, P., LODGE, D., AND NIELSEN, F. E. Quinoxalinediones: potent competitive non-NMDA glutamate receptor antagonists. *Science Wash. DC* 241: 701–703, 1988.

HORIKAWA, K. AND ARMSTRONG, W. E. A versatile means of intracellular labeling: injection of biocytin and its detection with avidin conjugates. *J. Neurosci. Methods* 25: 1–11, 1988.

HOTSON, J. R. AND PRINCE, D. A. A calcium-activated hyperpolarization follows repetitive firing in hippocampal neurons. *J. Neurophysiol.* 43: 409–419, 1980.

JONES, K. A. AND BAUGHMAN, R. W. NMDA- and non-NMDA-receptor components of excitatory synaptic potentials recorded from cells in layer V or rat visual cortex. *J. Neurosci.* 8: 3522–3534, 1988.

KANDEL, E. R. AND SPENCER, W. A. Electrophysiology of hippocampal neurons. II. After potentials and repetitive firing. *J. Neurophysiol.* 24: 242–259, 1961.

KAWAGUCHI, Y. AND HAMA, K. Two subtypes of non-pyramidal cells in rat hippocampal formation identified by intracellular recording and HRP injection. *Brain Res.* 411: 190–195, 1987.

KAWAGUCHI, Y. AND HAMA, K. Physiological heterogeneity of nonpyramidal cells in rat hippocampal CA1 region. *Exp. Brain. Res.* 72: 494–502, 1988.

KISVARDAY, Z. F., ADAMS, C. B. T., AND SMITH, A. D. Synaptic connections of axo-axonic (chandelier) cells in human epileptic temporal cortex. *Neuroscience* 19: 1179–1186, 1986.

KNOWLES, W. D. AND SCHWARTZKROIN, P. A. Local circuit synaptic interactions in hippocampal brain slices. *J. Neurosci.* 1: 318–322, 1981.

KOSAKA, T. The axon initial segment as a synaptic site: ultrastructure and synaptology of the initial segment of the pyramidal cell in the rat hippocampus (CA3 region). *J. Neurocytol.* 9: 861–882, 1980.

KOSAKA, T. Axon initial segments of the granule cell in the rat dentate gyrus: synaptic contacts on bundles of axon initial segments. *Brain Res.* 274: 129–134, 1983.

LACAILLE, J. C. Postsynaptic potentials mediated by excitatory and inhibitory amino acids in interneurons of stratum pyramidale of the CA1 region of rat hippocampal slices in vitro. *J. Neurophysiol.* 66: 1441–1454, 1991.

LACAILLE, J. C., KUNKEL, D. D., AND SCHWARTZKROIN, P. A. Electrophysiological and morphological characterization of hippocampal interneurons. In: *The Hippocampus—New Vistas,* edited by V. Chan-Palay and C. Köhler. New York: Liss, 1989, p. 287–305.

LACAILLE, J. C., MUELLER, A. L., KUNKEL, D. D., AND SCHWARTZKROIN, P. A. Local circuit interactions between oriens/alveus interneurons and CA1 pyramidal cells in hippocampal slices: electrophysiology and morphology. *J. Neurosci.* 7: 1979–1993, 1987.

LACAILLE, J. C. AND SCHWARTZKROIN, P. A. Stratum lacunosum-moleculare interneurons of hippocampal CA1 region. I. Intracellular response characteristics, synaptic responses, and morphology. *J. Neurosci.* 8: 1400–1410, 1988a.

LACAILLE, J. C. AND SCHWARTZKROIN, P. A. Stratum lacunosum-moleculare interneurons of hippocampal CA1 region. II. Intrasomatic and intradendritic recordings of local circuit synaptic interactions. *J. Neurosci.* 8: 1411–1424, 1988b.

LACAILLE, J. C. AND WILLIAMS, S. Membrane properties of interneurons in stratum oriens-alveus of the CA1 region of rat hippocampus in vitro. *Neuroscience* 36: 349–359, 1990.

LAMBERT, J. D. C. AND JONES, R. S. G. A reevaluation of excitatory amino acid-mediated synaptic transmission in rat dentate gyrus. *J. Neurophysiol.* 64: 119–132, 1990.

LANCASTER, B. AND ADAMS, P. R. Calcium-dependent current generating the afterhyperpolarization of hippocampal neurons. *J. Neurophysiol.* 55: 1268–1282, 1986.

LI, X. G., SOMOGYI, P., TEPPER, J. M., AND BUZSAKI, G. Axonal and dendritic arborization of an intracellularly labeled chandelier cell in the CA1 region of rat hippocampus. *Exp. Brain Res.* 90: 519–525, 1992.

LI, X. G., SOMOGYI, P., YILNEN, A., AND BUZSAKI, G. The hippocampal CA3 network: an in vivo intracellular labeling study. *J. Comp. Neurol.* 339: 181–208, 1994.

LLINAS, R. R. The intrinsic electrophysiological properties of mammalian neurons: insights into central nervous system functions. *Science Wash. DC* 242: 1654–1664, 1988.

MADISON, D. V. AND NICOLL, R. A. Control of the repetitive discharge of rat CA1 pyramidal neurones in vitro. *J. Physiol. Lond.* 354: 319–331, 1984.

MADISON, D. V. AND NICOLL, R. A. Enkephalin hyperpolarizes interneurones in the rat hippocampus. *J. Physiol. Lond.* 398: 123–130, 1988.

MARIN-PADILLA, M. The chandelier cell of the human visual cortex: a Golgi study. *J. Comp. Neurol.* 256: 61–70, 1987.

MAYER, M. L. AND WESTBROOK, G. L. The physiology of excitatory amino acids in the vertebrate central nervous system. *Prog. Neurobiol.* 28: 197–276, 1987.

MCCORMICK, D. A., CONNORS, B. W., LIGHTALL, J. W., AND PRINCE, D. A. Comparative electrophysiology of pyramidal and sparsely spiny stellate neurons of the neocortex. *J. Neurophysiol.* 54: 782–806, 1985.

MIHALY, A., ERDO, S. L., AND KUHNT, U. Time dependent loss of tissue GABA content and immunoreactivity in hippocampal slices. *Brain Res. Bull.* 26: 559–564, 1991.

MILES, R. Variation in strength of inhibitory synapses in the CA3 region of guinea-pig hippocampus in vitro. *J. Physiol. Lond.* 431: 659–676, 1990.

MILES, R. AND WONG, R. K. S. Unitary inhibitory synaptic potentials in the guinea-pig hippocampus in vitro. *J. Physiol. Lond.* 356: 97–113, 1984.

MISGELD, U. AND FROTSCHER, M. Postsynaptic-GABAergic inhibition of non-pyramidal neurons in the guinea-pig hippocampus. *Neuroscience* 19: 193–206, 1986.

MISGELD, U., MULLER, W., AND BRUNNER, H. Effects of (−)baclofen on inhibitory neurons in the guinea pig hippocampal slice. *Pfluegers Arch.* 414: 139–144, 1989.

NEWBERRY, N. R. AND NICOLL, R. A. A bicuculline-resistant inhibitory post-synaptic potential in rat hippocampal pyramidal cells in vitro. *J. Physiol. Lond.* 348: 239–254, 1984.

NEWBERRY, N. R. AND NICOLL, R. A. Comparison of the action of baclofen with γ-aminobutyric acid on rat hippocampal pyramidal cells in vitro. *J. Physiol. Lond.* 360: 161–185, 1985.

NICOLL, R. A., MALENKA, R. C., AND KAUER, J. A. Functional comparison of neurotransmitter receptor subtypes in mammalian central nervous system. *Physiol. Rev.* 70: 513–565, 1990.

OGATA, M. Physiological and pharmacological characterization of $GABA_B$ receptor-mediated potassium conductance. In: *$GABA_B$ Receptors in Mammalian Function,* edited by N. G. Bowery, H. Bittiger, and H.-R. Olpe. New York: Wiley, 1990, p. 273–291.

RAMON Y CAJAL, S. Estructura del asta de ammon y fascia dentata. *An. Soc. Esp. Hist. Nat.* 22: 53–114, 1893.

SAH, P., HESTRIN, S., AND NICOLL, R. A. Properties of excitatory postsynaptic currents recorded in vitro from rat hippocampal interneurones. *J. Physiol. Lond.* 430: 605–616, 1990.

SCHARFMAN, H. E. Dentate hilar cells with dendrites in the molecular layer have lower thresholds for synaptic activation by perforant path than granule cells. *J. Neurosci.* 11: 1660–1673, 1991.

SCHARFMAN, H. E. Differentiation of rat dentate neurons by morphology and electrophysiology in hippocampal slices: granule cells, spiny hilar cells and aspiny 'fast-spiking' cells. *Epilepsy Res.* 7, *Suppl.*: 93–109, 1992.

SCHARFMAN, H. E., KUNKEL, D. D., AND SCHWARTZKROIN, P. A. Synaptic connections of dentate granule cells and hilar neurons: results of paired intracellular recordings and intracellular horseradish peroxidase injections. *Neuroscience* 37: 693–707, 1990.

SCHARFMAN, H. E. AND SCHWARTZKROIN, P. A. Responses of cells of the rat fascia dentata to prolonged stimulation of the perforant path: sensitivity of hilar cells and changes in granule cell excitability. *Neuroscience* 35: 491–504, 1990.

SCHWARTZKROIN, P. A. AND KUNKEL, D. D. Morphology of identified interneurons in the CA1 regions of guinea pig hippocampus. *J. Comp. Neurol.* 232: 205–218, 1985.

SCHWARTZKROIN, P. A. AND MATHERS, L. H. Physiological and morphological identification of a nonpyramidal hippocampal cell type. *Brain Res.* 157: 1–10, 1978.

SCHWARTZKROIN, P. A. AND MUELLER, A. L. Electrophysiology of hippocampal neurons. In: *Cerebral Cortex. Further Aspects of Cortical Function, Including Hippocampus,* edited by E. G. Jones and A. Peters. New York: Plenum, 1987, vol. 6, p. 295–343.

SOMOGYI, P. A specific 'axo-axonal' interneuron in the visual cortex of the rat. *Brain Res.* 136: 345–350, 1977.

SOMOGYI, P. Synaptic organisation of GABAergic neurons and GABAA receptors in the lateral geniculate nucleus and visual cortex. In: *Neural Mechanisms of Visual Perception. Proceedings of the Retina Research Foundation Symposia,* edited by D. K.-T. Lam and C. D. Gilbert. The Woodlands, TX: Portfolio, 1989, vol. 2, p. 35–62.

SOMOGYI, P., FREUND, T. F., HODGSON, A. J., SOMOGYI, J., BEROUKAS, D., AND CHUBB, I. W. Identified axo-axonic cells are immunoreactive for GABA in the hippocampus and visual cortex of the cat. *Brain Res.* 332: 143–149, 1985.

SOMOGYI, P., NUNZI, M. G., GORIO, A., AND SMITH, A. D. A new type of specific interneuron in the monkey hippocampus forming synapses exclusively with the axon initial segments of pyramidal cells. *Brain Res.* 259: 137–142, 1983.

SOMOGYI, P. AND TAKAGI, H. A note on the use of picric acid-paraformaldehyde-glutaraldehyde fixative for correlated light and electron microscopic immunocytochemistry. *Neuroscience* 7: 1779–1783, 1982.

SORIANO, E. AND FROTSCHER, M. A GABAergic axo-axonic cell in the fascia dentata controls the main excitatory hippocampal pathway. *Brain Res.* 503: 170–174, 1989.

SORIANO, E., NITSCH, R., AND FROTSCHER, M. Axo-axonic chandelier cells in the rat fascia dentata: Golgi-electron microscopy and immunocytochemical studies. *J. Comp. Neurol.* 293: 1–25, 1990.

SPENCER, W. A. AND KANDEL, E. R. Electrophysiology of hippocampal neurons. III. Firing level and time constant. *J. Neurophysiol.* 24: 261–271, 1961.

STAFSTROM, C. E., SCHWINDT, P. C., CHUBB, M. C., AND CRILL, W. E. Properties of persistent sodium conductance and calcium conductance of layer V neurons from cat sensorimotor cortex in vitro. *J. Neurophysiol.* 53: 153–170, 1985.

STALEY, K. J., OTIS, T. S., AND MODY, I. Membrane properties of dentate gyrus granule cells: comparison of sharp microelectrode and whole-cell recordings. *J. Neurophysiol.* 67: 1346–1358, 1992.

STORM, J. F. Action potential repolarization and a fast after-hyperpolarization in rat hippocampal pyramidal cells. *J. Physiol. Lond.* 385: 733–759, 1987.

STORM, J. F. Potassium currents in hippocampal pyramidal cells. *Prog. Brain Res.* 83: 161–187, 1990.

SUTOR, B. AND HABLITZ, J. J. EPSPs in rat neocortical neurons in vitro. I. Electrophysiological evidence for two distinct EPSPs. *J. Neurophysiol.* 61: 607–620, 1989a.

SUTOR, B. AND HABLITZ, J. J. EPSPs in rat neocortical neurons in vitro. II. Involvement of *N*-methyl-D-aspartate receptors in the generation of EPSPs. *J. Neurophysiol.* 61: 621–634, 1989b.

TAUBE, J. S. AND SCHWARTZKROIN, P. A. Intracellular recording from hippocampal interneurons before and after development of long-term potentiation. *Brain Res.* 419: 32–38, 1987.

WITTER, M. P., GRIFFIOEN, A. W., JORRITSMA-BYHAM, B., AND KRIJNEN, J. L. M. Entorhinal projections to the hippocampal CA1 region in the rat: an underestimated pathway. *Neurosci. Lett.* 85: 193–198, 1988.

WONG, R. K. S. AND PRINCE, D. A. Participation of calcium spikes during intrinsic burst firing in hippocampal neurons. *Brain Res.* 159: 385–390, 1978.

WONG, R. K. S. AND PRINCE, D. A. Afterpotential generation in hippocampal pyramidal cells. *J. Neurophysiol.* 45: 86–97, 1981.